# MINISTRY OF NATIONAL EDUCATION TECHNICAL UNIVERSITY OF CIVIL ENGINEERING BUCHAREST DOCTORAL SCHOOL

# **REPORT NO 3**

# MONITORING OF GEOTECHNICAL STRUCTURES VALIDATION OF NUMERICAL CALCULATION MODELS

ing. Alexandru Poenaru

# **CUPRINS**

SYI	MBOLS	3
I	INTRODUCTION	6
II	MONITORING OF GEOTECHNICAL STRUCTURES	10
III	NUMERICAL METHODS IN GEOTECHNICAL ENGINEERING	15
IV	CASE STUDY - 3S+P+10E+ETH STRUCTURE	32
٧	CONCLUSIONS AND PERSPECTIVES	43
VI	BIBLIOGRAPHIES	49

# **Symbols**

The following symbols are used in this document:

#### A. Latin letters

- c cohesion
- c' effective cohesion
- cu undrained cohesion
- Cu undrained shear strength (obtained from DMT test)
- C<sub>v</sub> consolidation coefficient
- $c_{\alpha}$  coefficient of secondary compression
- $D_n$  particle size such that n% of the particle mass is less than that size  $D,\,e.g.$   $\,D_{10}$  ,  $D_{15}$  ,  $D_{30}$  ,  $D_{60}$  ,  $D_{85}$  .
- E Young's modulus of elasticity
- E' Young's modulus of elasticity drained
- E<sub>oed</sub> oedometer module
- Eu undrained modulus of elasticity Young
- E<sub>0</sub> the initial Young's modulus of elasticity
- $E_{50}$  Young's modulus of elasticity corresponding to 50% of maximum shear stress
- fs local friction on the friction mantle of a CPT cone
- Ic consistency index
- I<sub>D</sub> relative density
- I<sub>DMT</sub> material index based on flat dilatometer test
- I<sub>P</sub> plasticity index
- M<sub>DMT</sub> dilatometric modulus of elasticity
- $N_k$  cone factor in CPT static cone penetration test
- n number, e.g., number of trials or any numbers
- q<sub>c</sub> cone penetration resistance
- qt cone penetration resistance corrected for pore water pressure effects
- w natural humidity
- V<sub>s</sub> s-wave velocity
- V<sub>p</sub> p-wave velocity
- u pore water pressure

#### **B. Greek letters**

- γ density
- γ' submerged density
- $\sigma$  (z) the normal stress on a supporting structure at depth z
- $\sigma_{v0}$  total vertical effort
- $\phi$  angle of internal friction
- $\phi'$  angle of internal friction in terms of effective stresses
- $\zeta_f$  shear strength at normal stress

#### C. Abbreviations and abbreviations

- CAI Intermediate Clay Complex
- CPT cone penetration test
- $\mathsf{CPT}_\mathsf{U}$  static cone penetration test with pore water pressure measurement
- CU<sub>n</sub> direct shear test consolidated undrained under unsaturated conditions
- CU<sub>i</sub> direct shear test consolidated undrained under saturated conditions
- CD direct shear test consolidated drained
- DMT Marchetti Flat Dilatometer test
- DPL dynamic probing light
- DPM dynamic probing medium
- DPH dynamic probing heavy
- ED<sub>n</sub> oedometer test under unsaturated conditions
- ED<sub>i</sub> oedometer test under saturated conditions
- ED<sub>i300</sub> oedometer test under unsaturated conditions with sample flooding at 300 kPa pressure
- LB Bucharest Loam
- NPC Colentina sands and gravels
- MCPT static penetration with mechanical cone
- SPT standard penetration test
- UU direct unconsolidated-drained shear test



# D. The following units and their sub/multiples were used for the calculations

- strength kN - stress, pressure, strength, stiffness kPa - moment kNm - coefficient of permeability m/s - density (density)  $kg/m^3$  - consolidation factor  $m^2/s$  - density  $kN/m^3$ 

Note - The symbols used in this document are similar to those defined in SR EN 1990:2004 and conform to ISO 3898:2013.

#### I INTRODUCTION

The present Research report, entitled "Monitoring of geotechnical structures. Validation of numerical computational models", part of the Thesis "Correlations between geotechnical field tests and geotechnical soil parameters. Validation by monitoring the behavior of structures over time", consists of a presentation of the principles of geotechnical monitoring, modelling of soil structure interaction and a case study. In the case study, the geotechnical parameters obtained according to the correlations obtained and presented in Research Report 2 were used as input data. After the creation of the geotechnical numerical model, it was calibrated, through an iterative back-calculation analysis, using data obtained from the geotechnical time monitoring of a structure.

This chapter aims to give a brief overview of the whole research report. It will review the key points made in each chapter and the reasons why this report was necessary. As part of this introductory chapter, the typical stratification of the Bucharest area is summarized, with a presentation of the macro geotechnical characteristics of each layer. The investigated layers are "Bucharest Loam", "Colentina Sands and Gravels" and "Intermediate Clay Complex".

Today, in situ geotechnical investigation methods are experiencing an upward trend, exponentially, one could say, in their use, especially at national level. In practical terms, one can observe an alignment of geotechnical investigation methodologies in Romania with those present in the West. It should be noted that in the past in Romania there was an affinity for geotechnical laboratory tests, compared to the international situation where laboratory tests were correlated with in-situ investigations. Internationally, in-situ tests are increasingly developed, associated with the elaboration of technical standards based directly on their results.

Since in Romania the technical design standards are based on values of geotechnical parameters, the use of field tests requires the existence of correlations between the values measured in the field and the usual geotechnical parameters. There are numerous such correlations in the international literature, which have been elaborated and developed in the European Union, the United States and Japan. The existing correlations need to be validated or adapted to the specific soil types of our country. Although there are in practice also correlations determined in the past in Romania, their number is limited. Their limited existence leads to the under-potential use of field tests and to excessive caution in establishing characteristic and calculation values of geotechnical parameters.

This research report will present field and laboratory geotechnical investigations, geotechnical model creation using previously determined parameters using numerical methods (FEM), geotechnical monitoring during execution and operation, and *back-calculation* analyses to validate the model calculation. On the basis of the results obtained, useful conclusions can be drawn on the validity of the correlations used in the research report No 2 and, if necessary, the correlations will be corrected.

The final chapter presents the conclusions and perspectives of this research report.

#### I.1 Geotechnical description of the soil in Bucharest

The sites investigated for the purpose of this research report are located in Bucharest or in its immediate vicinity. From a **geomorphological point of view** (Figure I.1), the sites fall within the Bucharest Plain, located in the geomorphological subunit called the Colentina

Plain, part of the Vlăsiei Plain unit of the larger Romanian Plain unit. Towards the north-west, the Vlăsiei Plain has an altitude of 75-80 m and towards the south-east the altitude decreases to approx. 50 m.

This unit was formed morpho-genetically on fluviolacustrine-, alluvial-pluvial blankets of Pliocene-Quaternary age, mostly covered by clayey, sandy and alluvial (gravel) deposits. The hydrographic network in the area delimiting the Vlăsiei Plain is formed by the Colentina and Argeș rivers to the north and west and the Mostiștea to the east, with north-west-southeast courses, with riverbeds partly covered by marshes, partly transformed into lakes. The Bucharest plain has altitudes ranging from 100 -115 m in the north-west to 50 -60 m in the south-east, in the Dâmboviţa valley.

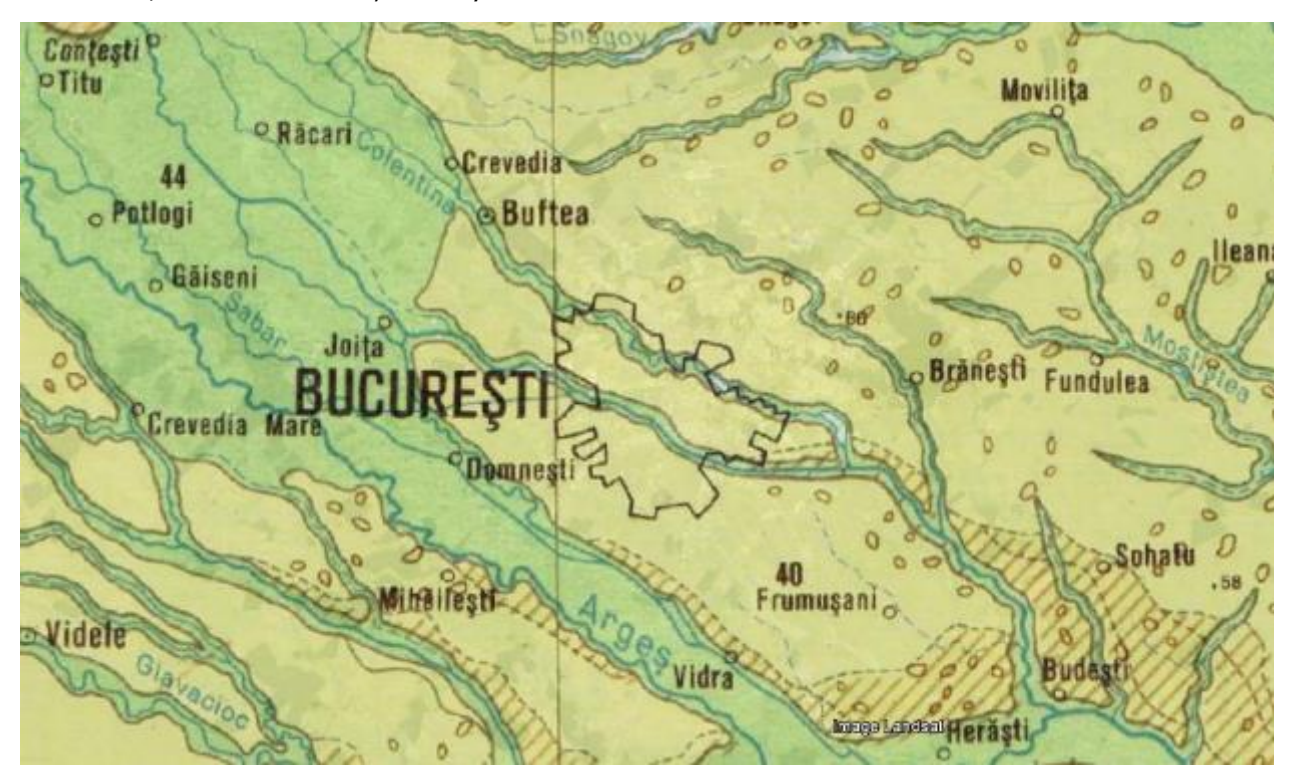


Figure I.1 - Morphology of the Bucharest area

**Geologically**, the sites are located in the northern part of the Moesic Platform, known as the Wallachian Platform. The geological deposits studied are of Quaternary age (Pleistocene  $q_p$ , Holocene -  $q_h$ ). These cover the whole region are about 300 -350 m thick and are composed from top to bottom of the geological formations described below.

On the surface there are old and new fills and recent alluvium (Holocene -  $q_h$ ), from the low terraces of the Dambovita river meadow (2 - 10 m thick).

The topsoil has largely been replaced/covered as a result of the development of the city. The infill is the result of intensive urbanization of the area over the last few hundred years. A significant part of it has been deposited as a result of the destruction caused by the Second World War, the industrialization and new town planning during the communist period and the 1977 earthquake. Fills can locally reach thicknesses of over 12-15 m.

The first natural layer is called the "Upper Sandy Clay Complex" or "Bucharest Loam" and consists of -silty-clay deposits in which lenses of clayey sands occure. In the central area

of the municipality this layer has undergone changes in thickness due to the settlement works of the last century. Locally, in the area of the former clay pits, this complex has completely disappeared. The upper sandy clay complex is an unsaturated layer over most of its thickness.

The upper sandy complex or "Colentina sands and gravels" is the second major layer intercepted in the Municipality area. The complex is composed of small sands and gravels (Upper Pleistocene age -  $qp_3$ ). The anthropic influence on this layer remains significant, due to the numerous works of systematization and exploitation of the aquifer.

The intermediate lacustrine complex also known as the 'Intermediate Clay Complex' is generally made up of clays or grey silty clays with sandy lenticular zones.

The intermediate sandy complex or "Mostistea Sands" is composed of medium to fine, medium to coarse sand, sometimes with clayey or silty interlayers (Upper Pleistocene age  $-qp_3$ ). They are composed of sands and fine sands and are found at depths between 20 and 50 m.

The next major layer is the 'Marl complex'. This is made up of clays and fine sands (the Coconi layers).

The Frătești layers are made up of sands and gravels with clay horizons. This layer represents the oldest Quaternary age formation in the area (Lower Pleistocene -  $qp_1$ ). The average depth of interception is relative (about 100 - 180 m).

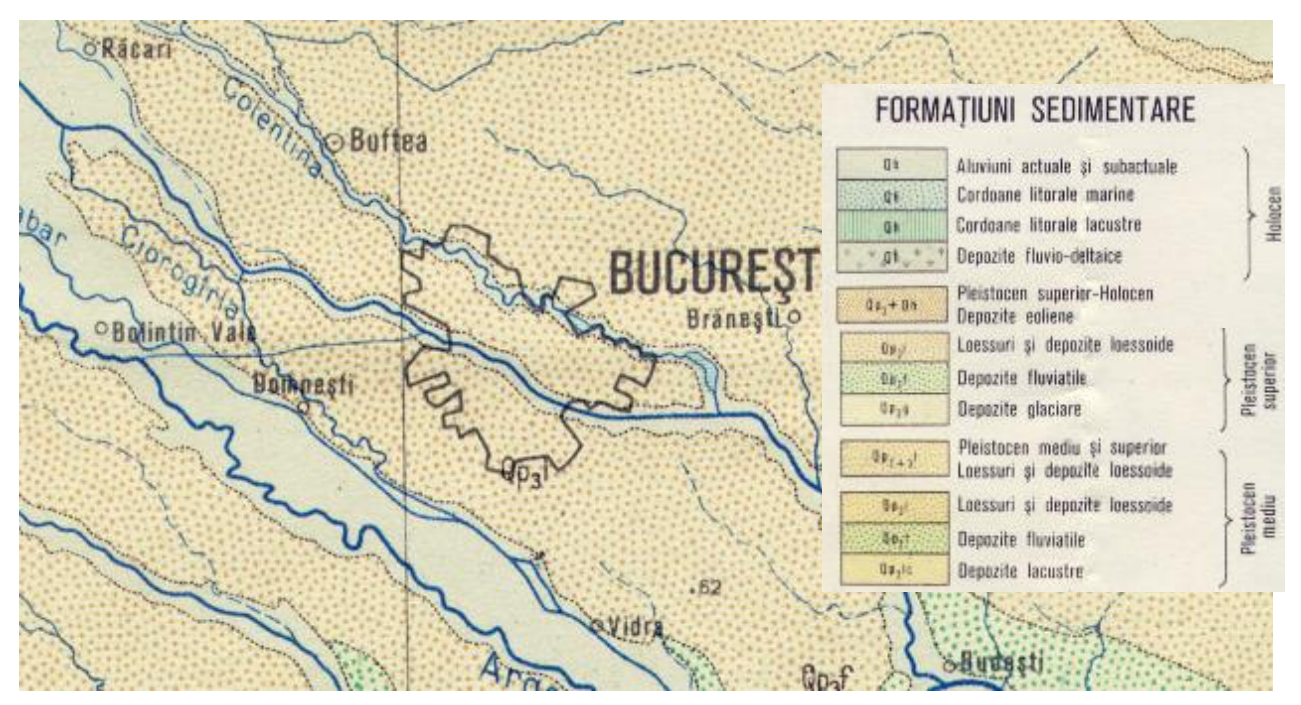


Figure I.2 - Geology of the investigated site

Numerous boreholes with depths of 200-300 m in Bucharest have shown that the formations in this area are made of different alluvium with very large variations in granularity, from gravels to clays, their stratification being lenticular or cross-bedded.

From a **hydrogeological point of view**, three aquifer systems are known to develop in the Bucharest area at the level of quaternary deposits.

The deepest aquifer system is known as the "Frătești strata" and consists of three sandy horizons (A, B and C horizons) separated by clay horizons. In the Bucharest area, the Frătești layers are found at depths between 80 m (in the southern part of the city) and 260 m (in the northern part of the city).

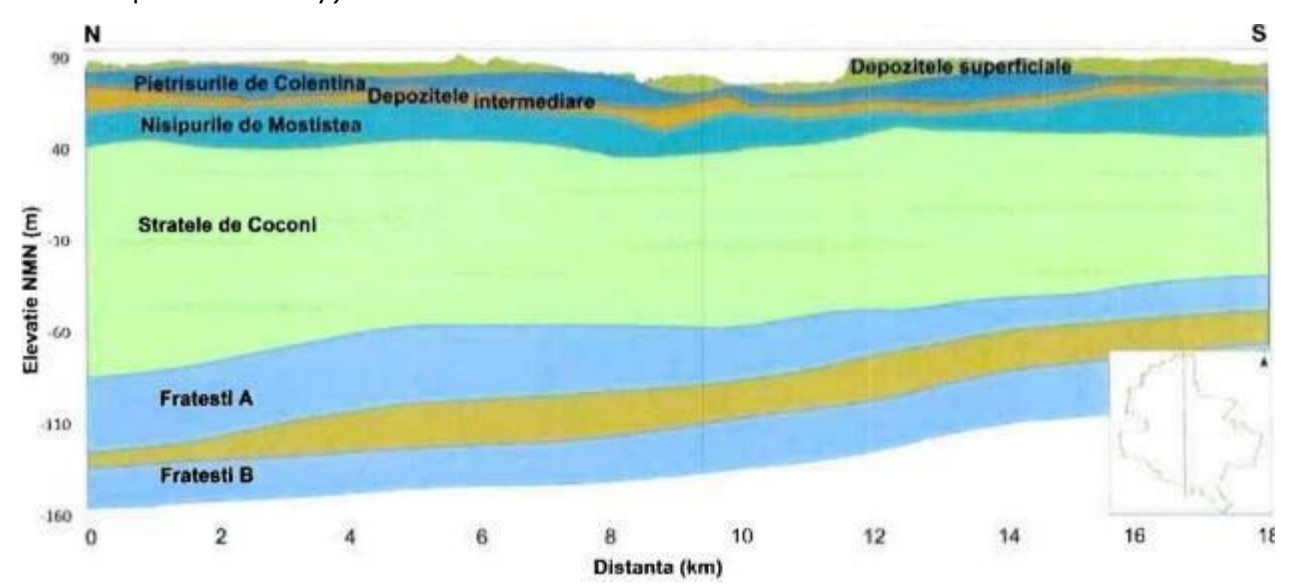


Figure I.3 - N-S Geological section of the Bucharest area

The second aquifer system is known by the name taken from the "Mostistea Sands". Groundwater flow in this layer is under pressure.

The third important aquifer layer called "Colentina gravels". The water flow in this aquifer is predominantly free level and has a direct interaction with the urban infrastructure of Bucharest. The variation of water levels in this aquifer depends on the functioning of the drainage system of the metro tunnel, water losses from the sewerage system, water drainage works, recharge from adjacent aquifers and the rainfall regime.

Groundwater in the Bucharest area has an active dynamic and a general direction of flow from northwest to southeast, as does the hydrographic network.

# II MONITORING OF GEOTECHNICAL STRUCTURES

"The justifiable uses of instrumentation are so many, and the questions which instruments and observations of them can answer, are so vital, that we should not risk discrediting their value by using them inappropriately or unnecessarily" - Ralph Peck (1984)

Geotechnical tools refer to tools used to monitor geotechnical projects or works requiring such monitoring. Geotechnical tools and monitoring are essential for the successful completion of geotechnical projects. Geotechnical monitoring work varies according to the degree of difficulty of the construction. They range from simple settlement monitoring to a wide range of monitoring tools when dealing with complex projects such as tunnels, landslides and deep excavations in urban areas.

Instrumentation of geotechnical structures is necessary for the evaluation of displacements and deformations of structures under real field conditions, as well as in the performance evaluation of new materials, methods and models used in the design and construction of geotechnical structures. Instruments that monitor ground deformation and displacements are mainly used for studies of slope stability, support structures, ground behavior during construction as well as after its completion.

Deep excavations in urban areas, inclinometers and topographic monitoring are used in almost all projects. It should also be noted that groundwater level monitoring can prove particularly important. In some projects, micro-deformation monitoring is important to deduce moments and axial forces in the structural element. Fixed-point extensometers are sometimes used to monitor the evolution of subsidence under the foundation of a structure. The methods by which geotechnical monitoring is carried out do not depend on the location and zoning of the ground but rather on the type of works.

#### II.1 Inclinometer measurements

Measurements are made by devices called inclinometer. Measurements are made by lowering the equipment to the base of the installed inclinometer columns installed in/near the structural element. Inclinometer measurements involve measuring displacements at successive intervals that can vary between 0.25 - 1 m. At each position the depth and inclination with respect to the vertical are recorded.

According to the technical data sheet of the usual manufacturers of inclinometer equipment, measurements are made with an accuracy of approx.  $\pm 0.5 - 1$  mm/10 m depth. The inclination of the inclinometer probe is determined digitally using MEMS technology, and the equipment allows inclination measurement in 2 orthogonal directions. Thus, tilt values are obtained in the plane determined by the probe wheels running on the groove of the pipe - the "A" axis and in the plane perpendicular to it - the "B" axis.

Typical components of the inclinometer measuring system are the inclinometer column, inclinometer probe, inclinometer cable and datalogger.

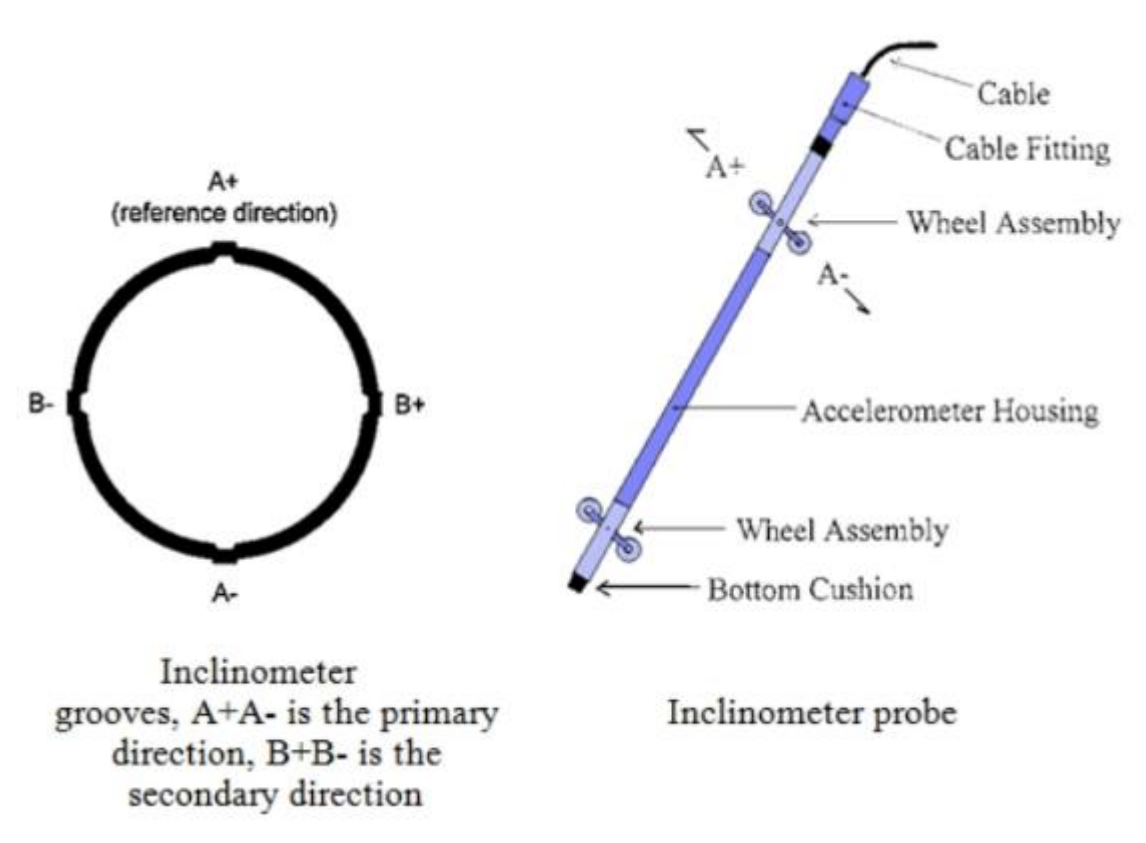


Figure II.1 - Operation of inclinometer equipment

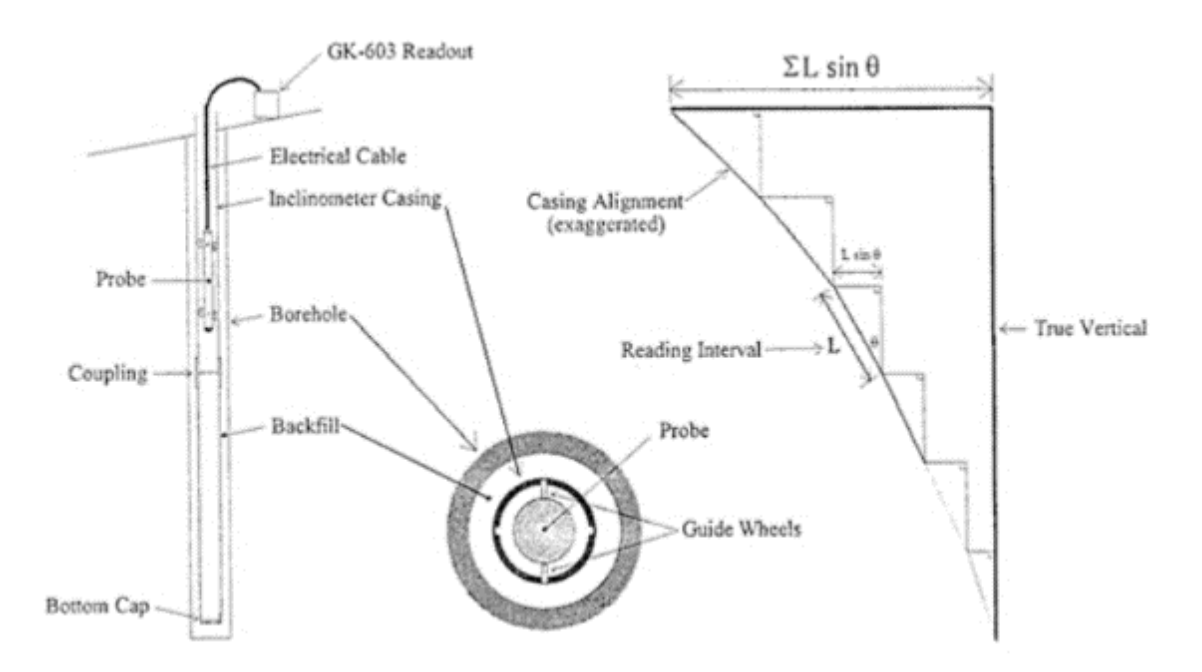


Figure II.2 - Installation of inclinometer equipment

After the installation of the inclinometer tubes in the structural element or in the soil mass, the first measurements will be made, which are generically called "0" reading or

reference reading. The assumption underlying the determination of the inclination of structures using the inclinometer considers the base of the inclinometer tube to be fixed, an assumption that must be verified at each cycle of inclinometer measurements.

# II.2 Groundwater level monitoring

If the groundwater level interacts with the future structure, it should be monitored. The groundwater level is measured in special columns, which can be installed both inside and outside the enclosure. Uncontrolled variations in groundwater levels can have negative consequences, which can even lead to reaching ultimate limit states, followed by collapse.



Figure II.3 - Groundwater level monitoring equipment

Knowing the upper elevation of the piezometric tube, it is possible to determine the groundwater level at the site relative to the elevation  $\pm 0.00$ . Groundwater level monitoring equipment usually provides a measurement accuracy of approx.  $\pm 1$  mm. The installation depths of piezometers outside the enclosure should be determined by the geotechnical design.



Figure II.4 - Pressure transducers

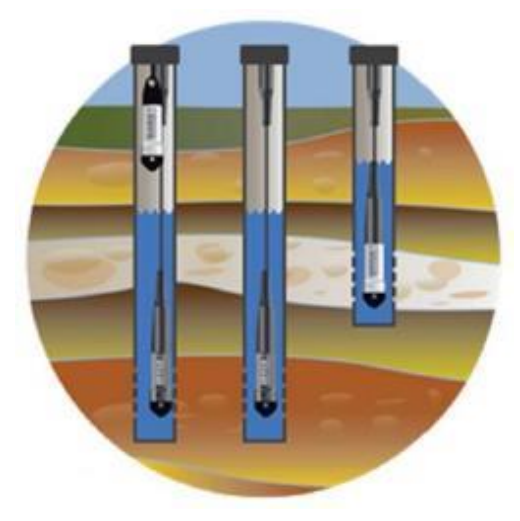


Figure II.5 - Installation principle of pressure transducers

Groundwater level measurements and monitoring can also be done continuously with digital devices (pressure transducers) with automatic recording. The advantage of these devices is that they allow monitoring of water pressure variation and compensation of atmospheric pressure differences, over a long period of time and at fixed, initially set time intervals. It is recommended to double the measurements, for verification purposes, with readings using an electronic level gauge. The sensors can be installed in the piezometric tubing after cleaning and cleaning the borehole.

#### II.3 ACCURACY AND VERTICALITY LEVELLING MEASUREMENTS

In order to carry out the work of monitoring the behavior over time of the structures of the buildings adjacent to the site, a planimetric and levelling base network must be created. Three GPS points outside the area of influence of the works on the site must be determined.

The monitoring of construction settlements by topographic methods consists of monitoring the evolution of the elevations of isolated points, materialized by settlements marks and related to reference landmarks (also called fixed landmarks).

The tamping markers are mobile levelling markers, which are made of stainless-steel rods and are fixed to adjacent building elements and networks, to kerbs and pavements of adjacent access routes, to the raft, to the diaphragm walls, to the crown beams, floors and pillars of the construction, in such a way as to ensure their preservation over time for the entire duration of the observations and to make it possible to carry out measurements both during construction and during operation.



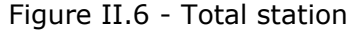




Figure II.7 - High precision level

A levelling device is used to perform precision geometric levelling on the tamping marks. For a high level of accuracy, it is recommended to use an electronic levelling device with bar code reading. The accuracy provided by this equipment shall be class B, according to STAS 2745-90, tab. 1. Fixed points in the local network must be included in the levelling network.

A-mark for determining the verticality of the facade of a diaphragm wall, using reflective targets, must be materialized in the field by two reflective targets, mounted as a pair, at



different heights on the wall of the buildings, one at the top of the facade wall and one at the bottom. The following reasoning can be used to determine the verticality of the walls.

At time i, from a point having known x and y coordinates in the Stereo70 system, aim at the targets mounted on the building in question. By joining the points given by the x and y coordinates of the two targets a line will be obtained, which will be used as a reference for the following readings. At time Ti+1 the above procedure will be repeated and a new line will be obtained by joining the points given by the new x and y coordinates of the same targets.

The accuracy provided by the equipment used to measure distances is 0.77 mm + 0.970  $\times$  10-6 m  $\times$  D - distance in mm.

The limitation of the use of inclinometers is due to the principle of the method, which involves measuring only horizontal deformations of the ground. Inclinometers are essential for monitoring movements within the soil mass (not just on the surface), especially for works involving slope stabilization and deep excavations.

# III Numerical methods in geotechnical engineering

Soil is a complex material with non-linear, anisotropic behavior that varies with time when subjected to stress. Typically, it behaves differently under loading, unloading and reloading. Under loading, the soil undergoes plastic deformation and its stiffness is dependent on the level of loading. The soil also exhibits different stiffness in the range of very low strain loads. These aspects cannot be taken into account by modelling the behavior of the soil using simple elastic constitutive models.

A constitutive model is a mathematical formulation of the mechanical behavior of a given material. This mathematical formulation is represented by stress-strain relations, with the link between the equilibrium and compatibility equations being integrated.

The actual mechanical behavior of soils is complex, characterized by a strong anisotropic character. The current level of knowledge in this field does not yet admit a unitary constitutive law that fully captures this complex behavior. However, a number of deformation laws have been developed over time, simulating the mechanical behavior of soils through linear elastic (Hooke), elasto-plastic (Mohr-Coulomb), hyperbolic (Duncan & Chang) or non-linear elastic (hyper-elastic, hypo-elastic) relations.

In his work (Brinkgreve, 2005) details five aspects that are necessary to describe the behavior of a soil type. These are briefly presented below. The first aspect to be considered is the influence of water on the behavior of a soil, in terms of effective stresses and pore water pressures. The second aspect is related to the influence on the stiffness of a soil, the level of loading, the stress path (loading and unloading), the level of deformations, the density, the permeability of the soil, the level of consolidation and the anisotropy. Irreversible deformations caused by loading must be taken into account, which is the third aspect. The fourth aspect focuses on factors that influence the strength of a soil, such as loading rate, age and type of drainage. Other factors that also need to be taken into account are the level of compaction, expansion and the memory of the consolidation effort.

#### III.1 DEFINITION OF STRESSES AND STRAINS

In the Cartesian coordinate system, the effort can be expressed as a tensor defined by the following matrix:

$$[\sigma] = \begin{bmatrix} \sigma_{x} & \sigma_{xy} & \sigma_{xz} \\ \sigma_{yx} & \sigma_{y} & \sigma_{yz} \\ \sigma_{zx} & \sigma_{zv} & \sigma_{z} \end{bmatrix}$$

The meaning of the efforts that make up the matrix is given in Figure III.1, below.

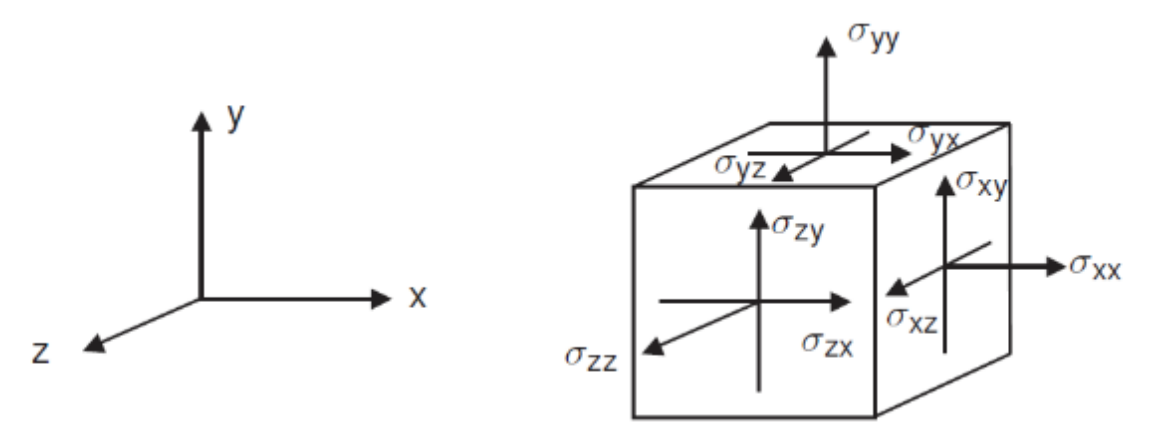


Figure III.1 - General coordinate system and sign convention for efforts

Given that the stress tensor is symmetric, it follows that  $\sigma_{xy} = \sigma_{yx}$ ,  $\sigma_{yz} = \sigma_{zy}$  and  $\sigma_{zx} = \sigma_{xz}$ . Thus, the effort can also be written in vector form with a number of six components:

$$\sigma = (\sigma_{x} \sigma_{y} \sigma_{z} \sigma_{xy} \sigma_{yz} \sigma_{zx})^{T}$$

Figure III.1 shows the positive components of normal stress, considered as strains. The negative components of normal stress indicate compression on the element. The constitutive model is generally expressed by a relationship between an infinitesimal increment of stress producing an infinitesimal increment of strain.

Most of the time, for simplicity of relationships, one can resort to using principal efforts instead of Cartesian components in the constitutive model. The principal stresses are in fact the values of the stress tensor when the tangential stresses are zero.

Deformation, similar to strain in the Cartesian coordinate system is represented by the following matrix:

$$[\varepsilon] = \begin{bmatrix} \varepsilon_{x} & \varepsilon_{xy} & \varepsilon_{xz} \\ \varepsilon_{yx} & \varepsilon_{y} & \varepsilon_{yz} \\ \varepsilon_{zx} & \varepsilon_{zy} & \varepsilon_{z} \end{bmatrix}$$

Analytically, deformation is the derivative of the displacement component. According to the theory of small deformations the sum of the complementary components  $\epsilon_{ij}$  and  $\epsilon_{ji}$  produced by tangential stresses is called tangential strain, denoted by  $\gamma$ .

Taking into account the conditions stated in the case of defining the stress and strain can be defined in vector form with the tangential strain components as follows:

$$\boldsymbol{\epsilon} = \left( \boldsymbol{\epsilon}_{x} \, \boldsymbol{\epsilon}_{y} \, \boldsymbol{\epsilon}_{z} \, \boldsymbol{\gamma}_{xy} \, \boldsymbol{\gamma}_{yz} \, \boldsymbol{\gamma}_{zx} \right)^{\top}$$

#### III.2 CONSTITUTIVE MODELS WITH APPLICATION IN GEOTECHNICS

Soil is a non-linear behaving material with a strong anisotropic but also rheological character when subjected to loading. In general, soils behave differently when subjected to primary loading, unloading and reloading. All these aspects need to be implemented in a set of mathematical equations that adequately simulate this behavior.

Over the years, numerous constitutive models have been developed, each with corresponding advantages and limitations that depend largely on the area of applicability. In evaluating a model in terms of its applicability, three essential aspects are considered (Chen, 1985). The first aspect refers to the theoretical evaluation with respect to the compliance with the basic principles of mechanics, considering the requirements of continuity, stability and uniqueness. A second evaluation parameter is the ability of a model to incorporate parameters that can easily be obtained by standard laboratory tests. In this way the input data used in the numerical modelling can be validated. A third criterion is the ease of implementation of the constitutive model in numerical modelling. In other words, this last aspect refers to the adaptation of the model to the computing power of existing processors.

#### III.2.1 Linear elastic model

The linear elastic model is the simplest constitutive model requiring only two input parameters, E, or elasticity modulus, and  $\upsilon$ , or Poisson's ratio. This model is based on Hooke's law and the relationship between stress and strain is linear. The applicability of this model in geotechnics, especially in numerical modelling, is quite limited due to the non-linear behavior of the soil. The relationship between stress and strain is expressed as:

$$\sigma = M \cdot \epsilon$$

# III.2.2 Elasto-plastic model (Mohr-Coulomb)

The Mohr-Coulomb model is a plastic perfect elastic model usually used for a first-order approximation of the soil behavior. This model is an extension of the elastic model, therefore using the same parameters, plus a yield criterion defined by the parameters  $\phi$  and c, i.e., the internal friction angle and the cohesion of the material concerned.

The Mohr-Coulomb model of failure is an extension of Coulomb's law of friction to general stress and strain states. In fact, this condition ensures compliance with Coulomb's law in any plane in a material. The complete Mohr-Coulomb yielding model - contains six flow functions which are formulated in terms of effective stresses below.

$$f_{1a} = \frac{1}{2} (\sigma'_2 - \sigma'_3) + \frac{1}{2} (\sigma'_2 + \sigma'_3) \sin \varphi - c \cos \varphi \le 0$$

$$f_{1b} = \frac{1}{2} (\sigma'_3 - \sigma'_2) + \frac{1}{2} (\sigma'_3 + \sigma'_2) \sin \varphi - c \cos \varphi \le 0$$

$$f_{2a} = \frac{1}{2} (\sigma'_3 - \sigma'_1) + \frac{1}{2} (\sigma'_3 + \sigma'_1) \sin \varphi - c \cos \varphi \le 0$$

$$f_{2b} = \frac{1}{2} (\sigma'_1 - \sigma'_3) + \frac{1}{2} (\sigma'_1 + \sigma'_3) \sin \varphi - c \cos \varphi \le 0$$

$$f_{3a} = \frac{1}{2} (\sigma'_{1} - \sigma'_{2}) + \frac{1}{2} (\sigma'_{1} + \sigma'_{2}) \sin \varphi - c \cos \varphi \le 0$$

$$f_{3b} = \frac{1}{2} (\sigma'_{2} - \sigma'_{1}) + \frac{1}{2} (\sigma'_{2} + \sigma'_{1}) \sin \varphi - c \cos \varphi \le 0$$

Two plastic parameters occurring in the flow functions are well known,  $\phi$  - the angle of internal friction and c - cohesion.

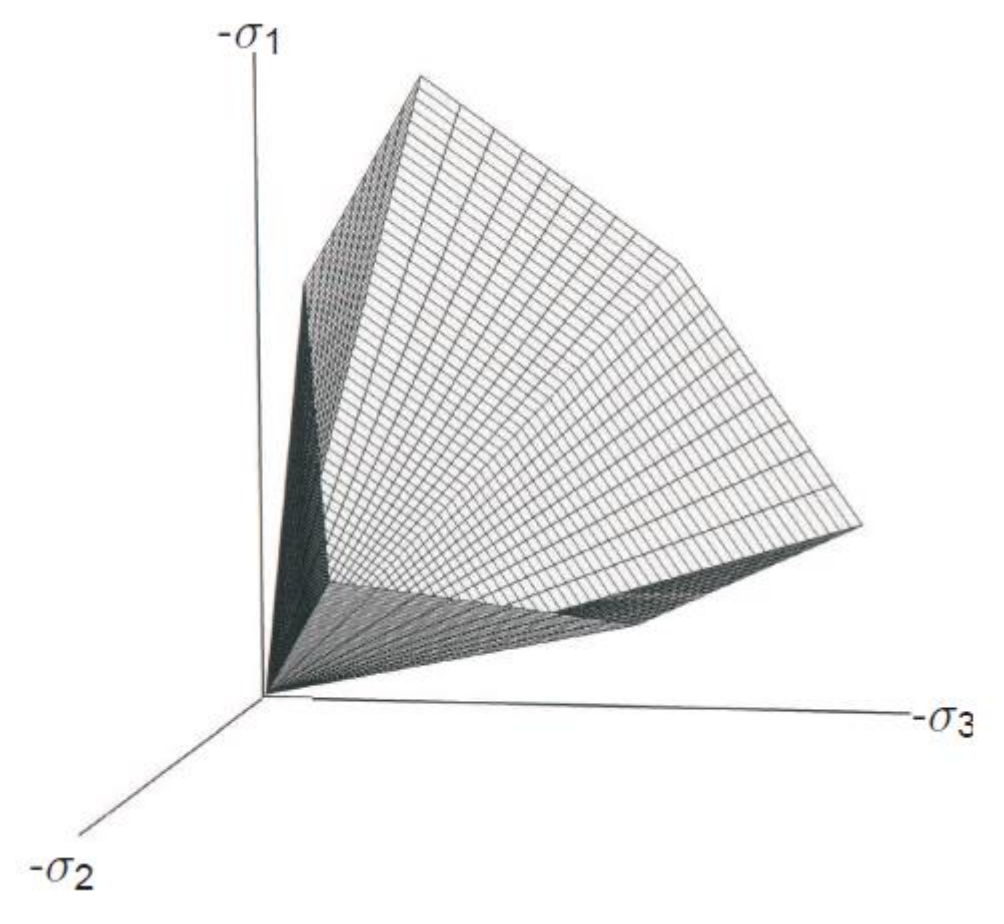


Figure III.2 - Mohr-Coulomb yield surface in principal stress space

#### III.2.2.1 Main parameters of the Mohr-Coulomb model

The linear elastic perfect plastic Mohr Coulomb model needs five parameters, which are easy to obtain and are commonly used in geotechnical engineering. These parameters can be obtained from common geotechnical tests and are listed below:

E: Young's module;

v: Poisson coefficient;

c: cohesion;

φ: angle of internal friction;

#### ψ: angle of expansion.

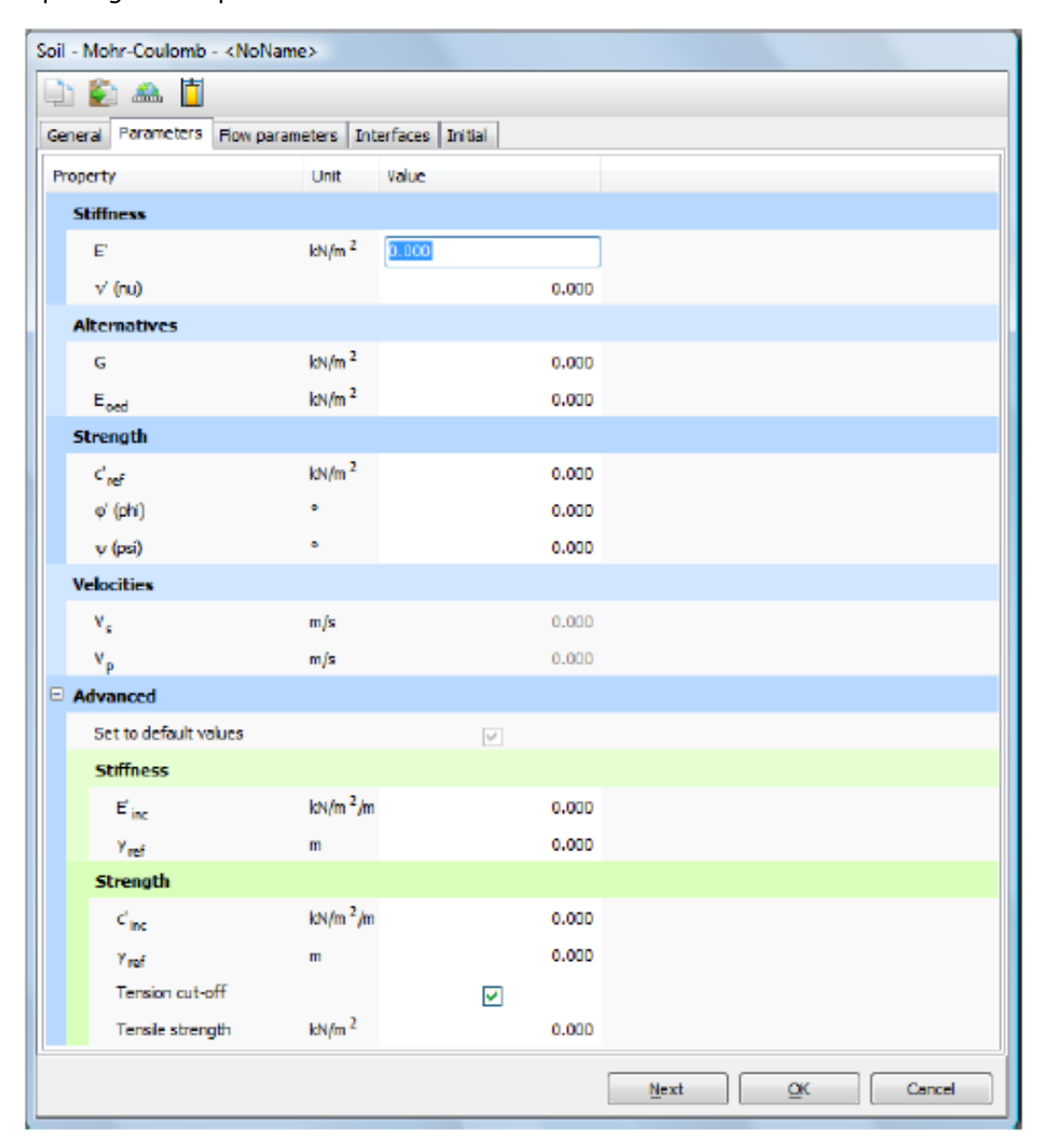


Figure III.3 - Table with input parameters for the Mohr-Coulomb model in Plaxis

For applications in the dynamic domain or as an alternative in the absence of parameters, the following parameters can also be used in numerical analysis:  $v_p$  and  $v_s$ .

#### III.2.2.2 Young's modulus (E)

Plaxis uses Young's modulus as the main parameter for stiffness in the elastic model and in the Mohr-Coulomb model. The values of the stiffness parameter chosen in the modeling require special attention since many natural materials have non-linear behavior from the beginning of loading. In a triaxial test of soils, the initial slope of the stress-strain curve (tangent modulus) is usually  $E_0$ , and the secant modulus at 50% strength is defined as  $E_{50}$ . For materials with predominantly elastic behavior, it is best to use  $E_0$ , while for soils, for a more accurate assessment  $E_{50}$  is generally used. In problems involving modelling the behavior after unloading of the soil in question, the module  $E_{UR}$  (unload-reload) is used instead of  $E_{50}$ . For

soils in general  $E_{UR}$  and  $E_{50}$  tend to increase with the confining pressure. Thus, soils at depth tend to have higher stiffness than in surface layers.

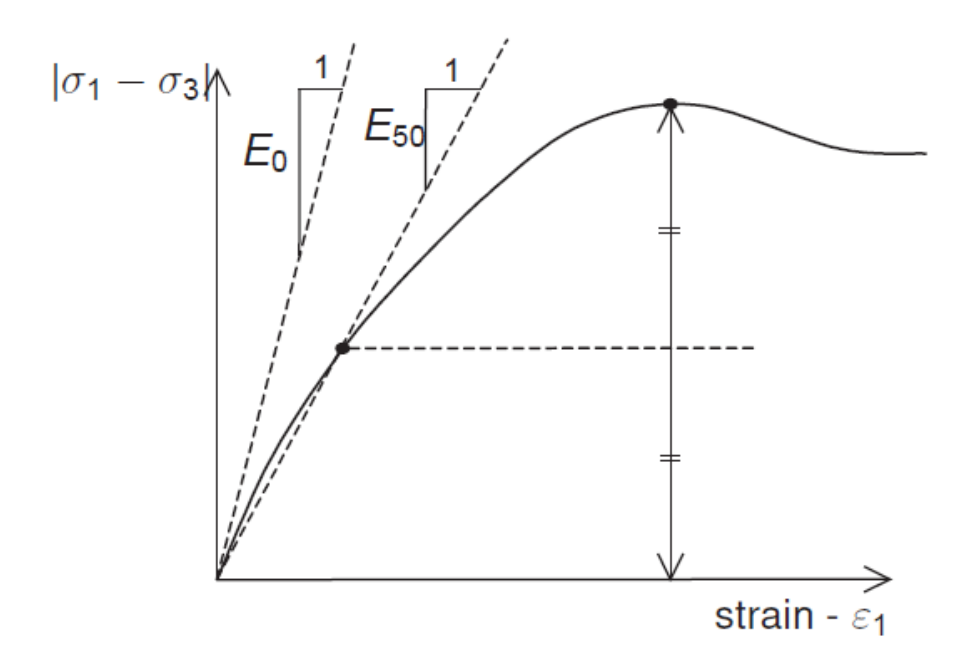


Figure III.4 - Definition of E<sub>0</sub> and E<sub>50</sub> for a standard triaxial test

#### III.2.2.3 Poisson's ratio ( $\nu$ )

In a drained triaxial test a significant volume deformation may occur at the beginning of the axial test and thus a reduced value of the initial Poisson's ratio  $\nu_0$ . For some cases, especially unloading problems, it may be more realistic to use a lower initial value, but in general when using the Mohr-Coulomb model is recommended to use a higher value.

Choosing the correct Poisson's ratio when using the Plaxis program is generally straightforward due to the loads that are generally applied gravitationally. This type of loading provides values closer to reality for  $K_0$ .

#### III.2.2.4 Cohesion (c)

Cohesion is measured by effort. In the Mohr-Coulomb constitutive model, the cohesion parameter can be used to model effective cohesion  $c^\prime$  in combination with an effective friction angle  $\phi^\prime$ .

The advantage of using effective parameters to model soil behavior is that the change in shear strength with reinforcement is achieved automatically. However, it is recommended to check the state of stress after consolidation.

Plaxis can model totally non-cohesive c=0 soils, but in some cases errors may occur. To avoid possible errors in numerical analysis, for soil layers close to the ground surface a very low cohesion c>0.2 kPa can be used. Also, a special option is implemented in the software where cohesion increases with depth.

#### III.2.2.5 Angle of internal friction (φ)

The angle of internal friction is entered in degrees. In general, the internal friction angle is used to model the internal friction of a soil in combination with the effective cohesion c'. This can be obtained for both drained and undrained (A) modelling.

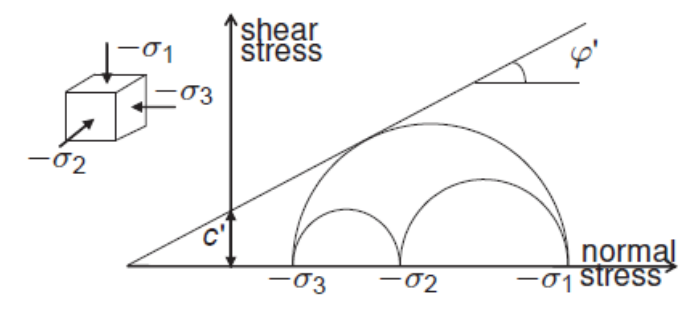


Figure III.5 - Use of drained parameters

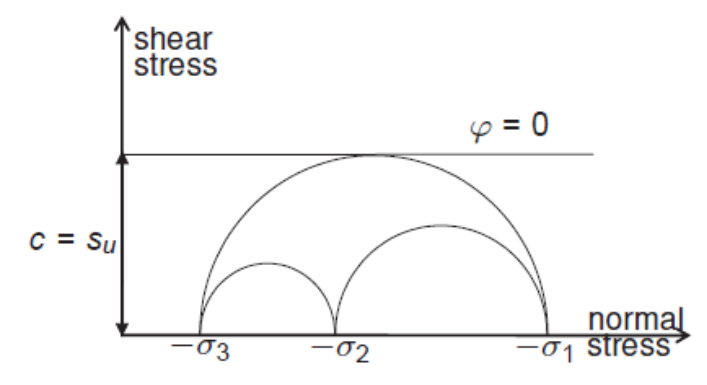


Figure III.6 - Use of undrained parameters

Internal friction angles with high values are generally obtained for very coarse sands. These will increase the plastic computational effort. The calculation time increases approximately exponentially with the internal friction angle. Thus, too high internal friction angles should be avoided in the preliminary analysis. It is preferable not to use angles greater than 35 degrees in such situations.

#### III.2.2.6 Shear modulus (G)

The shear modulus, G, is measured in terms of effort. According to Hook's law, the relationship between Young's modulus E and shear modulus G is as follows:

$$G = \frac{E}{2(1+\nu)}$$

Introducing a value for one of the alternatives G or  $E_{\text{oed}}$  results in E changing while the Poisson coefficient remains constant.

#### III.2.2.7 Oedometer modulus Eoed

The oedometer modulus,  $E_{\text{oed}}$ , has effort as its unit of measurement. According to Hook's law, the relationship between Young's modulus, E and the oedometer modulus,  $E_{\text{oed}}$  is as follows:

$$E_{oed} = \frac{(1 - \nu)E}{(1 - 2\nu)(1 + \nu)}$$

# III.2.3 Hyperbolic model

The hyperbolic model is also called the "Duncan and Chang" model, after its developers. Starting from the relationship below formulated by Kodner (1963), based on the results of compression tests in the triaxial apparatus, the two developed this model by introducing into the model formulation the dependence of stiffness on stress level.

$$(\sigma_1 - \sigma_3) = \frac{\varepsilon}{a + b \cdot \varepsilon}$$

- σ<sub>1</sub> și σ<sub>3</sub> is the maximum or minimum main effort;
- ε is the axial deformation;
- a is the initial tangent strain modulus;
- b is the inverse of the value of the deviatoric effort.

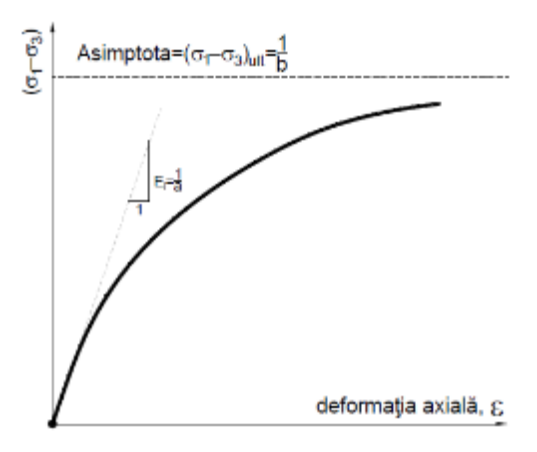


Figure III.7 - Stress-strain curve in hyperbolic model

The yield criterion for the hyperbolic model is based on the Mohr-Coulomb criterion. Its peculiarity compared to the elastic-perfect-plastic model is that it captures the most important characteristics of soils behavior under stress, namely: non-linearity of the stress-strain relationship, stiffness as a function of stress level and inelastic behavior of cohesive and non-cohesive soils. This model is often used due to its advantages compared to the previously discussed constitutive models, however its formulation does not take into account the effect of dilatancy. Another major disadvantage is that it does not distinguish between loading and unloading. Therefore, it is not suitable for plastic stresses near the yield surface.

# III.2.4 The "Hardening Soil" model

The limitations of the hyperbolic model are addressed by the "hardening soil" model (Schanz et al. 1999), seen as an improvement on the latter. The main advantage of this model is the use of two flow surfaces (plastic deformations): the flow surface or volume roughening and the deviatoric roughening surface.

Compared to the elastic perfect-plastic (Mohr-Coulomb) model, the yield surface is not fixed in the principal stress space, but can be extended due to the occurrence of plastic deformations. It is necessary to differentiate between the two types of stiffening (stiffening = hardening) introduced by this model. Shear (deviatoric) stiffening and volume compression stiffening. Deviatoric hardening is due to irreversible deformations caused by primary deviatoric loads, while compression hardening is due to plastic deformations in isotropic or volumetric compression.

As shown by Kodner and later by Duncan and Chang, the relationship between stress and strain is well approximated by a parabola, especially in the case of triaxial loading. The features by which the "hardening soil" model is an improvement of the hyperbolic model are the following: the relations are based on plasticity theory instead of elasticity theory, the dilatancy phenomenon is included and a second roughening surface is introduced.

#### III.2.4.1 Constitutive equations

The stress-strain relationship resulting from a standard triaxial test can be approximated by the following hyperbolic relationship:

$$\epsilon_1 = \; \frac{1}{2 \cdot E_{50}} \, \frac{q}{1 - q \, / \; q_a} \, , \quad \; q \, < \, q_f \label{epsilon}$$

- $\epsilon_1$  is the vertical deformation of the specimen;
- q<sub>a</sub> is the asymptotic value of the shear strength;
- q<sub>f</sub> represents the ultimate deviatoric effort (at break);
- q is the deviatoric (shear) effort;
- $\bullet$  E<sub>50</sub> is the state-dependent stiffness modulus corresponding to the mobilization of 50% of the shear strength.

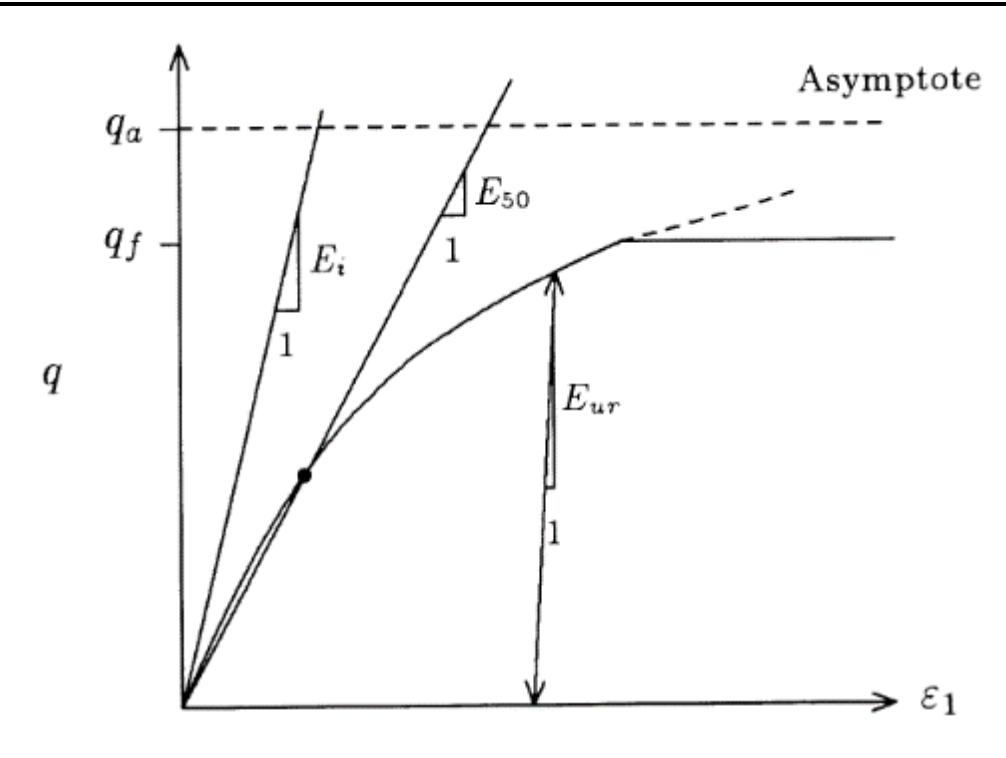


Figure III.8 - Use of undrained parameters Stress-strain curve corresponding to the standard triaxial test

Asymptotic deviatoric and failure effort are expressed by the following relations:

$$q_f = \frac{6 \sin \phi}{3 - \sin \phi} (p + c \cot \phi)$$
 
$$q_a = \frac{q_f}{R_f}$$

- $p = \sigma_1 \sigma_3$ ;
- φ si c; shear parameters
- R<sub>f</sub> is the ratio of the deflection effort to the failure effort, usually equal to 0.9;

#### III.2.4.2 Primary load stiffness

The behavior of the soil under primary loads has a strong non-linear character. Parameter  $E_{50}$  is the stiffness modulus dependent on the confining stress under primary loading. The use of this modulus is preferred because the tangent modulus is more difficult to determine experimentally in the small deformation range. Modulus  $E_{50}$  is described by the following relation:

$$E_{50} = E_{50}^{ref} \left( \frac{c \cos \varphi - \sigma_3 \sin \varphi}{c \cos \varphi + p^{ref} \sin \varphi} \right)^{m}$$

in which  $p^{ref}$  is the reference confining pressure, and  $E_{50}^{ref}$  is the reference modulus.

The stress stiffness dependence is introduced by the parameter "m". The literature (Janbu, 1963; Soos, 1980) provides various values for this parameter, between 0.5 and 1.0 depending on the nature of the soil.

#### III.2.4.3 Rigidity for unloading/reloading

For unload-load stress roads, a different stiffness mode is required depending on the stress condition. This module, similar to the  $E_{50}$  is explained according to the relation below.

$$E_{ur} = E_{ur}^{ref} \left( \frac{c \cos \varphi - \sigma_3 \sin \varphi}{c \cos \varphi + p^{ref} \sin \varphi} \right)^m$$

The unloading-reloading stress path is modeled elastically non-linearly. Using Hooke's law relations, within this constitutive model, the elastic components of the deformation  $(\varepsilon_1^e, \varepsilon_2^e, \varepsilon_3^e)$  according to the following relations:

$$G_{\rm ur} = \frac{1}{2(1 + U_{\rm ur})} E_{\rm ur}$$

$$\epsilon_1^e = \frac{q}{E_{ur}} \, , \quad \epsilon_2^e = \, \epsilon_3^e = \, \upsilon_{ur} \frac{q}{E_{ur}} \label{epsilon}$$

It should be noted that these conditions are imposed on deformations that develop under deviatoric loading, while deformations arising in the first stage of loading are not taken into account.

# III.2.4.4 Hyperbolic function defined in the "hardening soil" model

To simplify the relationships, it is necessary to impose the conditions from the standard triaxial apparatus test, i.e.  $\sigma_2 = \sigma_3$  and  $\sigma_1$  is the maximum compressive stress. It should be noted that the triaxial test is of the drained type. Therefore, the stresses considered in the relations are effective stresses, without taking into account the pore water pressure. For the definition of the function, it is necessary to consider plastic deformations.

$$f = \bar{f} - \gamma^p$$

where  $\bar{f}$  is a stress function based on axial strain  $\epsilon_1$  and  $\gamma^p$  is the plastic strain.

$$\bar{f} = \frac{1}{E_{50}} \frac{q}{1 - q/q_a} - \frac{2q}{E_{ur}}$$

For primary loading f=0, so  $\bar{f}=\gamma^p$ . This gives the following equation, which defines the axial strain as the sum of the elastic and plastic components:

$$\epsilon_1 = \epsilon_1^e + \epsilon_1^p \cong \frac{1}{2 E_{50}} \frac{q}{1 - q / q_a}$$

Since it is a model expressing plasticity, "Hardening soil" implies a relationship between plastic deformations like the one below:

$$\epsilon_v^p \ = sin \ \psi_m \ \cdot \ \gamma^p$$

where  $\psi_m$  is the mobilised expansion angle, defined in terms of the internal friction angle specific to the critical state.

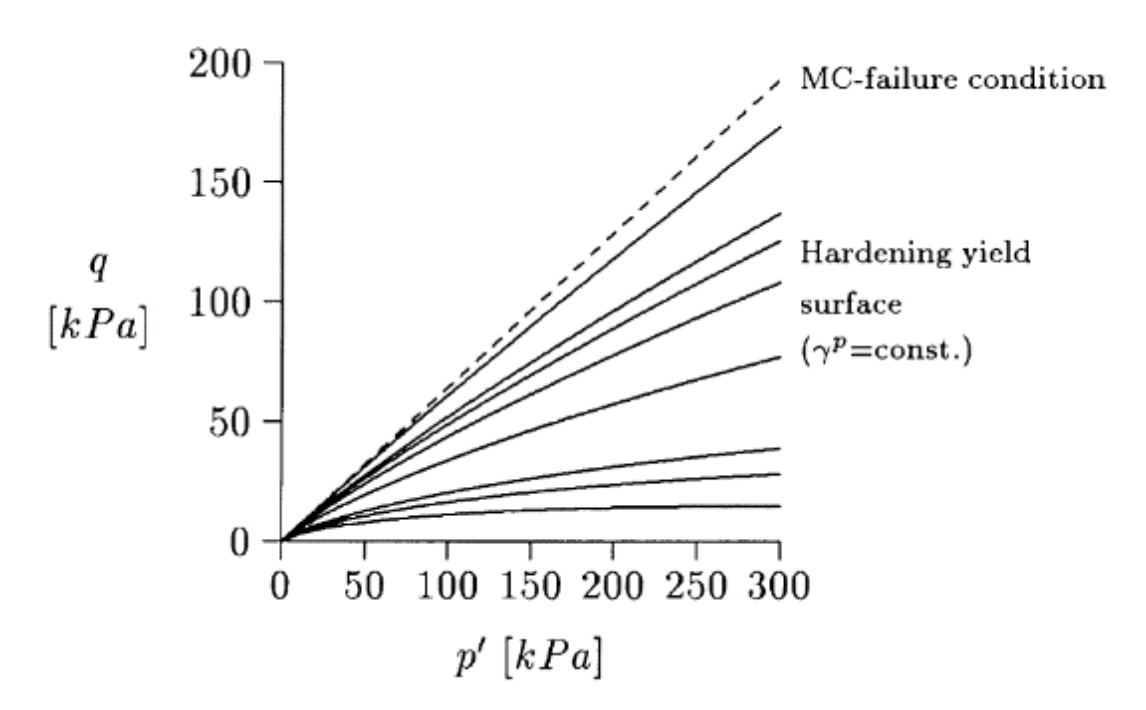


Figure III.9 - Hardening lines for constant values of the roughening parameter  $\gamma_\text{P}$ 

In Figure III.9, the hardening lines are plotted for different values of the plastic volume strain in p-q coordinates. In order to capture also the deformation recorded during isotropic compression, it is necessary to introduce a second flow surface bounding the elastic region in the direction of the p-coordinate. This surface is defined by the following equation:

$$f^c = \frac{\tilde{q}^2}{\alpha^2} + p^2 - p_p^2$$

in which:

- $\alpha$  is an auxiliary parameter related to the coefficient of soil at rest;
- $p = (\sigma_1 + \sigma_2 + \sigma_3) / 3;$
- $\tilde{q}$  is a special measure of deviatoric effort  $\tilde{q} = \sigma_1 + (\delta 1)\sigma_2 \delta\sigma_3$ ;
- $\delta = (3 \sin\varphi)/(3 + \sin\varphi)$ .

The maximum volume deformation before yielding is the limited plastic deformation in isotropic compression. In Figure III.10 can be seen the yield curves defining the "Hardening soil" model.

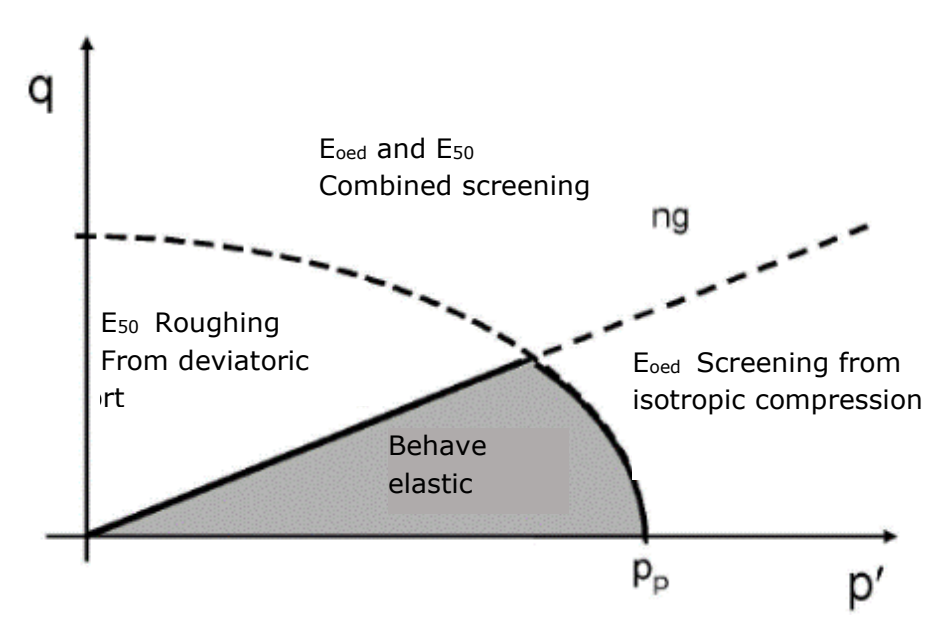


Figure III.10 - Hardening soil model yield curves

Both the deviatoric and the volume flow surface seen in plan according to the Mohr-Coulomb yield criterion have a hexagonal shape. Figure III.10 shows the graphical representation of the total flow surface area or cross-section of the Hardening soil model in the principal stress space, for a non-cohesive soil (c = 0).

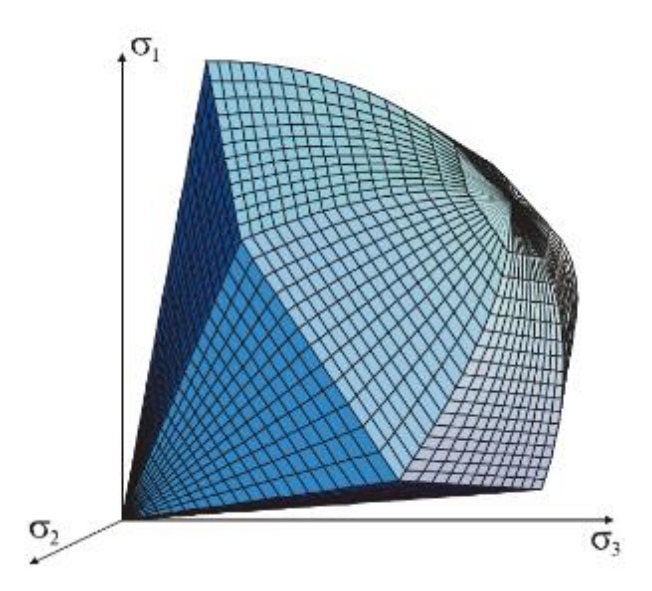


Figure III.11 - Graphical representation of the total flow area for the Hardening soil model

# III.2.5 Model Hardening Soil with Small-Strain Stiffness

The Hardening Soil model assumes elastic behavior of the material during loading and unloading respectively. However, the range of deformations in which the soil behaves perfectly elastically is very small. With increasing strain amplitude, the stiffness of the soil decreases

non-linearly. Figure III.12 shows the stiffness reduction curve with respect to strain level. Geotechnical applications and corresponding deformations are also shown.

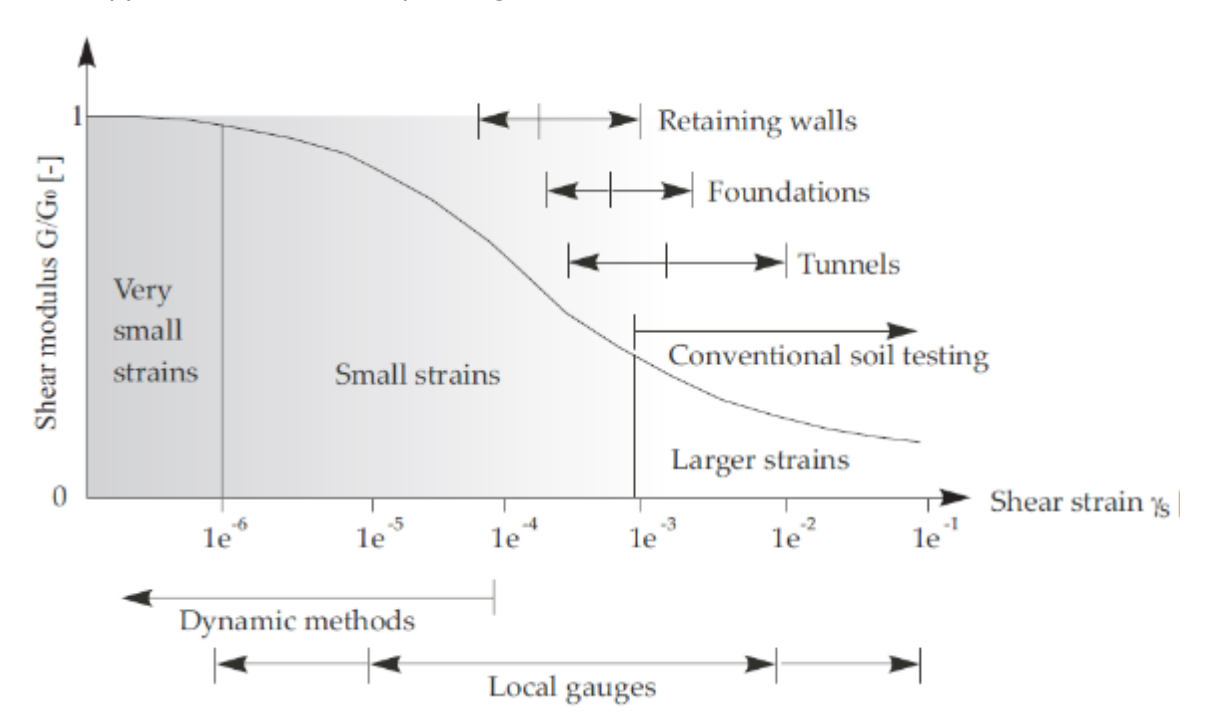


Figure III.12 - Stiffness-strain behavior of a soil type (Atkinson and Sallfors, 1991)

Stiffness at very small deformations and non-linear dependence on strain amplitude are considered in the Hardening Soil with Small-Strain model. For the description of this model, in addition to the Hardening Soil model, parameters  $G_0$  - the initial modulus of stiffness at very small deformations and  $\gamma_{0,7}$ , the level at which the shear modulus  $G_s$  is reduced to 70% of  $G_0$  are required.

# III.2.6 Modified Cam-Clay model

In the formulation of the Cam-Clay model, a logarithmic relationship between the pore index e and the mean value of the effective stress p' is assumed for the initial loading, which is expressed as:

$$e - e^0 = -\lambda ln \left(\frac{p'}{p^0}\right)$$

The parameter  $\lambda$  is the isotropic compression index, which characterizes the compressibility of a material during initial loading. The graph of the above relation in e - ln(p') coordinates is a straight line. The relation below is used to characterize the behavior during unloading and reloading:

$$e - e^{0} = -k ln \left( \frac{p'}{p^{0}} \right)$$

The parameter k, called the swelling index, characterizes the behavior of the material during unloading and reloading and represents a straight line. An infinite number of lines p' - e can be determined, corresponding to values of the pre-consolidation stress  $p_p$ .

The flow function defined for the modified Cam-Clay model is expressed as follows:

$$f = \frac{q^2}{M^2} + p'(p' - p_p)$$

The flow surface (f = 0) is plotted in the p' - q plane as an ellipse. This represents the limit of elastic behavior. Stress paths inside this curve are characterized by strain increases in the elastic domain, while curves beyond this curve are characterized by deformations in both the elastic and plastic domains. In the p' - q plane, the ellipse intersects at the top a line that can be expressed mathematically:

$$q = Mp'$$

This line is called the CSL critical state line and describes the relationship between p' and q at the limit state. The pre-consolidation effort,  $P_p$ , denotes the size of the ellipse, resulting in an infinite number of ellipses each corresponding to a value of  $P_p$ .

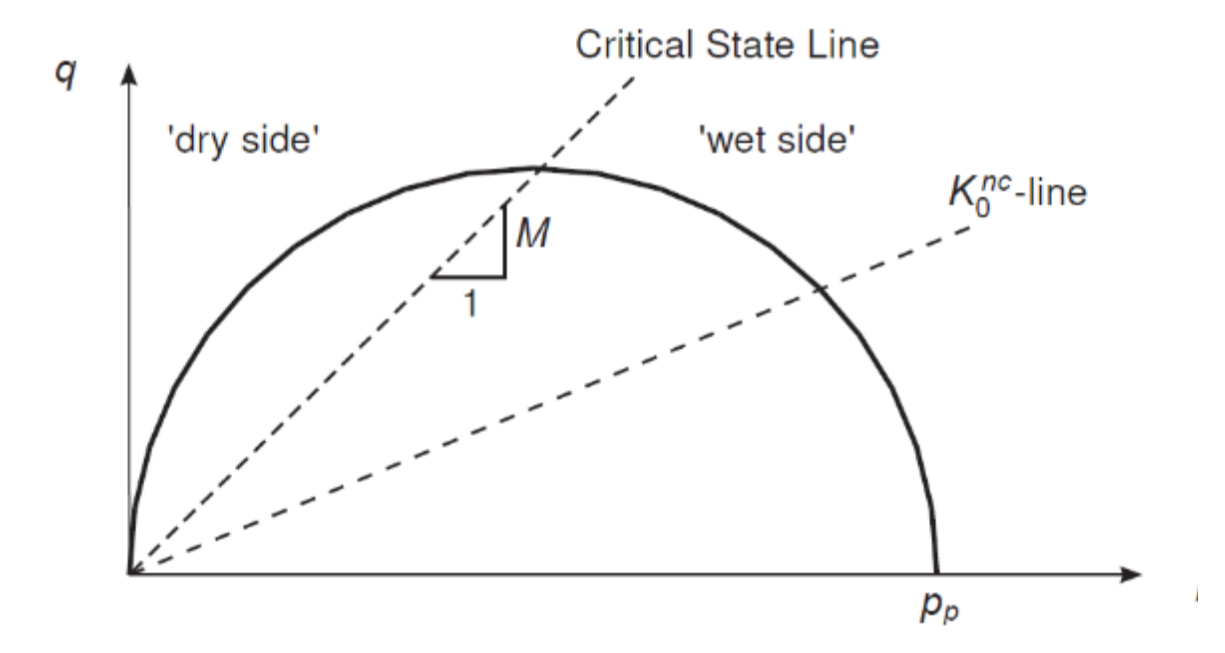


Figure III.13 - Yield surface of the modified Cam-Clay model in p' - q coordinates

In geotechnical modelling in the dynamic domain, when using the modified Cam-Clay model, the value of the k-index must be carefully chosen so that the model can correctly estimate the value of the shear wave velocity of the soil in question. This model is not recommended to be used in practical applications, since in the absence of experience it may create convergence problems in iterative processes.

#### III.2.7 Soft Soil Model

The soils that can be described using the soft soil model are clays approaching the normally consolidated condition, clayey silts and peat. High compressibility is the common feature of these models. The classification of materials in this category can be done by compressibility tests in an oedometer, by determining deformation moduli at a vertical stress of 100 kPa. The values of strain moduli  $E_{\text{oed}}$  range from 1 to 4 MPa, depending on the type of soil.

In general, the constitutive Hardening Soil model is used to model the behavior of compressible soils, with very good results in current practice. Soft soil is used in situations where soils are very compressible, e.g.,  $E_{\text{oed}}$  /  $E_{\text{50}}$  < 0.5.

The features of this constitutive model are as follows. Deformability is dependent on the load level with logarithmic progression, primary loading behavior is different from unloading-reloading behavior and the yield criterion according to Mohr-Coulomb.

The relationship between the volume deformation  $\epsilon_{v}$  and the average effective stress p' is described by a logarithmic curve which can be expressed as a function of the moment of loading (primary loading (equation 1) or unloading-reloading (equation 2).

$$\varepsilon_{v} - \varepsilon_{v}^{0} = -\lambda ln \left( \frac{p' + c \cot \varphi}{p^{0} + c \cot \varphi} \right) \tag{1}$$

$$\varepsilon_v^e - \varepsilon_v^{e0} = -k \ln \left( \frac{p' + c \cot \varphi}{p^0 + c \cot \varphi} \right) \tag{2}$$

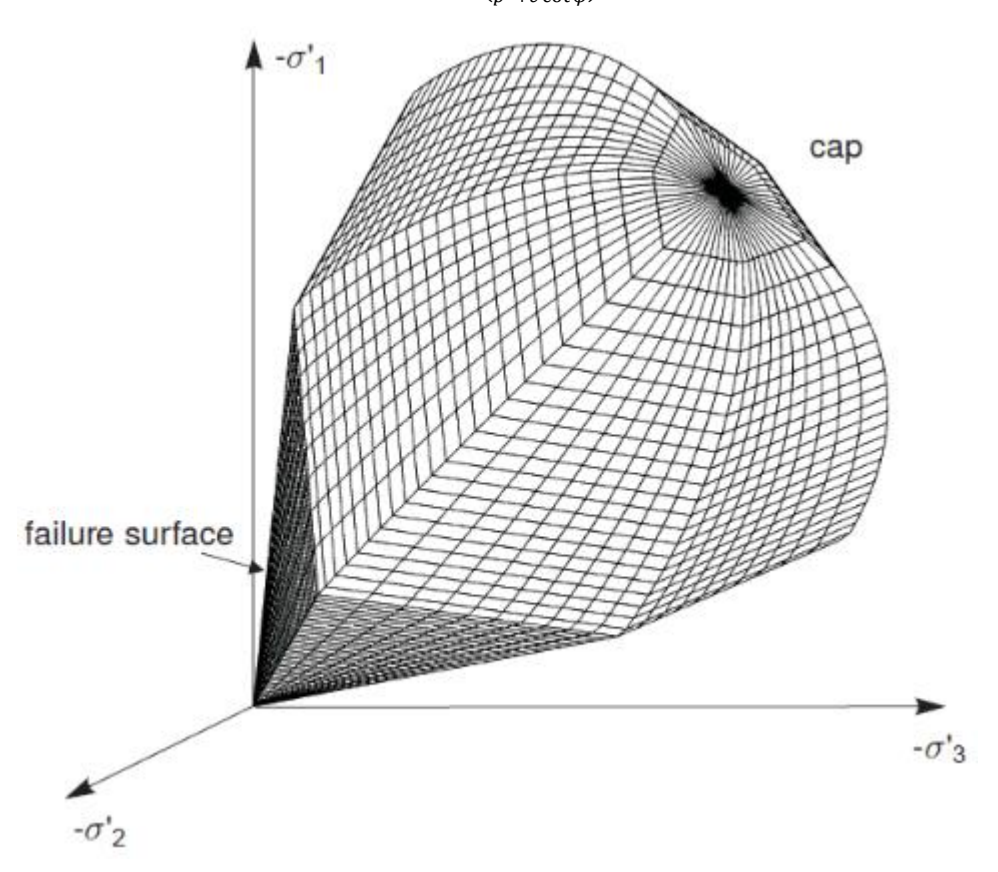


Figure III.14 - Total yield area of the Soft Soil model in the principal stress space

The Soft Soil constitutive model is used to model as closely as possible the behavior of highly compressible soils and can give results closer to real measurements than using classical models.

#### III.2.8 Conclusions on constituent models

Constitutive models are essential in modelling soil behavior for current geotechnical design. Over time, numerous models have been developed, from the simplest to the most complex. These are based on complex equations that attempt to describe the behavior of the



soil as faithfully as possible. The choice of a particular model for the design of a geotechnical structure has to be made with great care as more complex models do not necessarily give results that are closer to reality and experience of the user becomes important. For the use of more complex models, parameters are needed, which are obtained from more laborious and sensitive operator mode tests.

# IV Case study - Structure 3S+P+10E+Eth

#### IV.1 Introduction

This chapter presents a case study of a deep excavation located in the central western part of Bucharest. The depth-height regime is 3S+P+10E+Eth. The plot has an area of about  $5.000~m^2$  and has a polygonal shape. The main function of the new building will be offices and underground parking.

In the figure below, the plan of the deep excavation is shown together with the 3 sections that will be modeled.

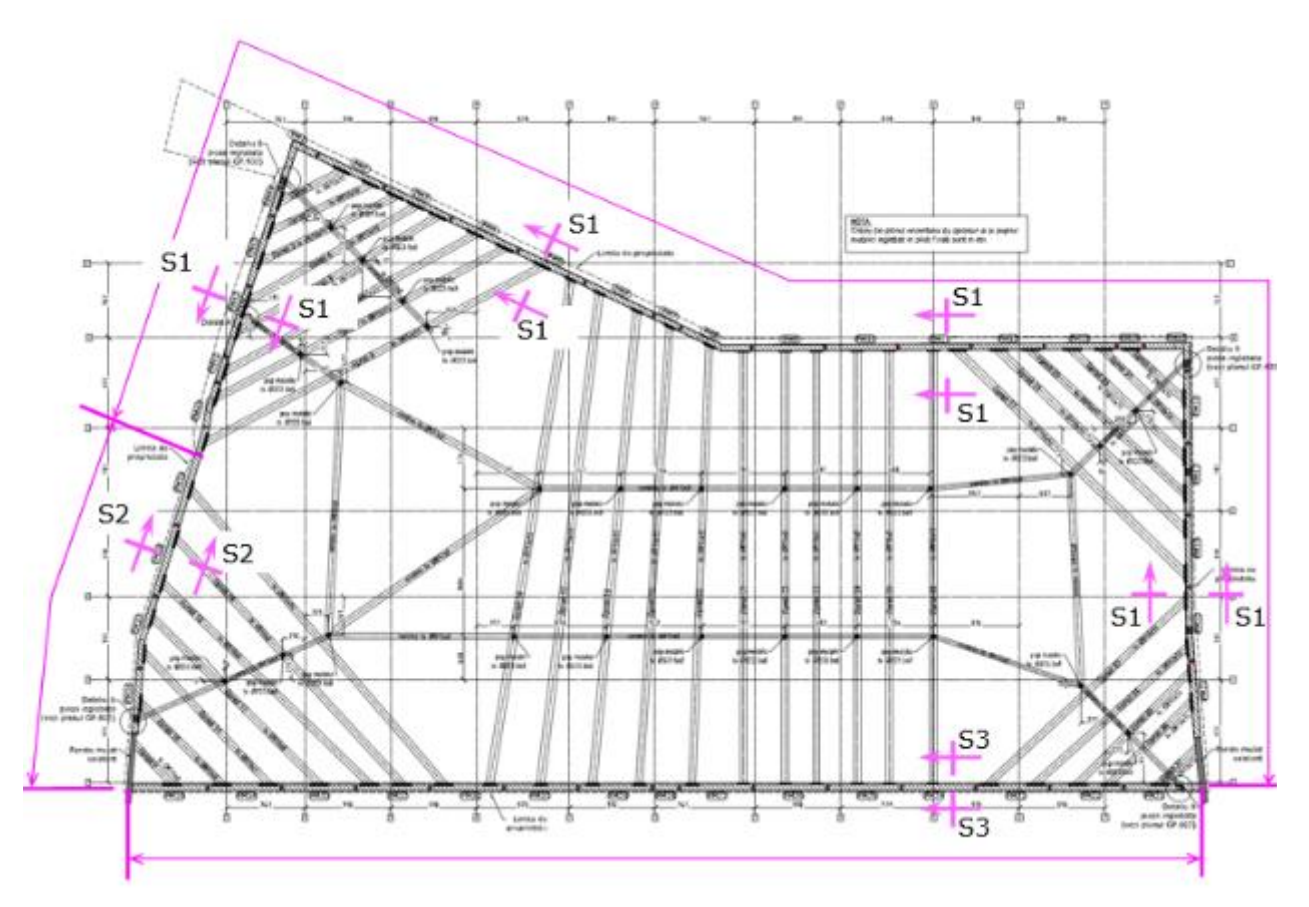


Figure IV.1 - Overview of designed works and design sections

# IV.2 Geotechnical parameters of the bedrock

On the basis of geotechnical investigations carried out on site, as well as data from our own archive, the characteristic geotechnical parameters were established.

The geotechnical investigations carried out to determine the geotechnical parameters required for the proposed analysis consisted of two geotechnical boreholes, three static penetrations with an electric cone (CPT) and two tests with a Marchetti flat-plate dilatometer equipped with a seismic module (SDMT).

The table below summarizes the analysis regarding the classification of the work in the geotechnical category according to NP074-2014. Based on this and on SR-EN-1997-1:2004,

the analyzed site is classified in the moderate geotechnical risk class, which corresponds, according to NP 074-2014, to geotechnical category 2.

Table IV.1. Geotechnical category of the analyzed project

Risk factor	Risk class	Score according to NP 074
Field conditions	Average land	3
Groundwater	With normal euphoria	2
Importance of construction	Normal	3
Neighborhood	Moderate risk	3
Seismic risk	a <sub>g</sub> ≥0.25g	3
Geotechnical risk	Moderate	14
Geotechnical category	2	

# IV.3 Geotechnical structure modelling

For the modelling of the soil structure interaction, an enclosure made of diaphragm walls (diaphragm walls) with a thickness of 60 cm and base at elevation -16.10/-17.00 was considered. The horizontal support of the panels of diaphragm walls will be made at elevation -5.00 by means of a top down with slabs spaced at  $\sim$ 4 m. The foundation solution adopted is that of direct foundation on the general raft.

#### IV.4 Excavation and foundation system modelling stages

The following is a schematic presentation of the stages of modelling the interaction of the structure ground

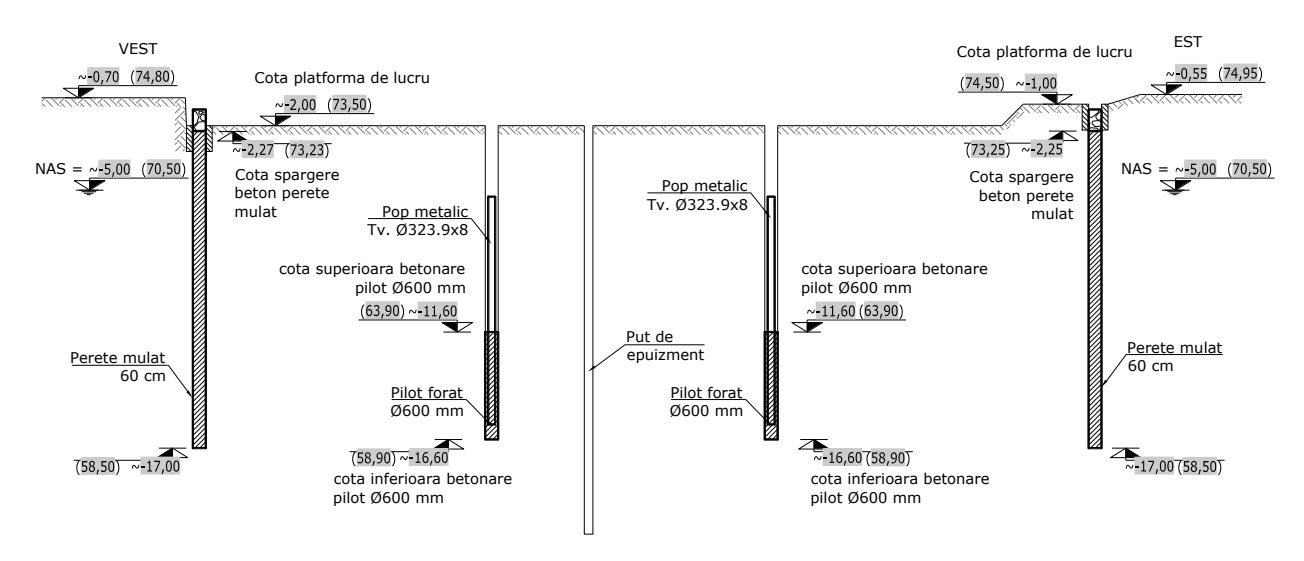


Figure IV.2 - Execution stage 1 - Creation of diaphragm walls

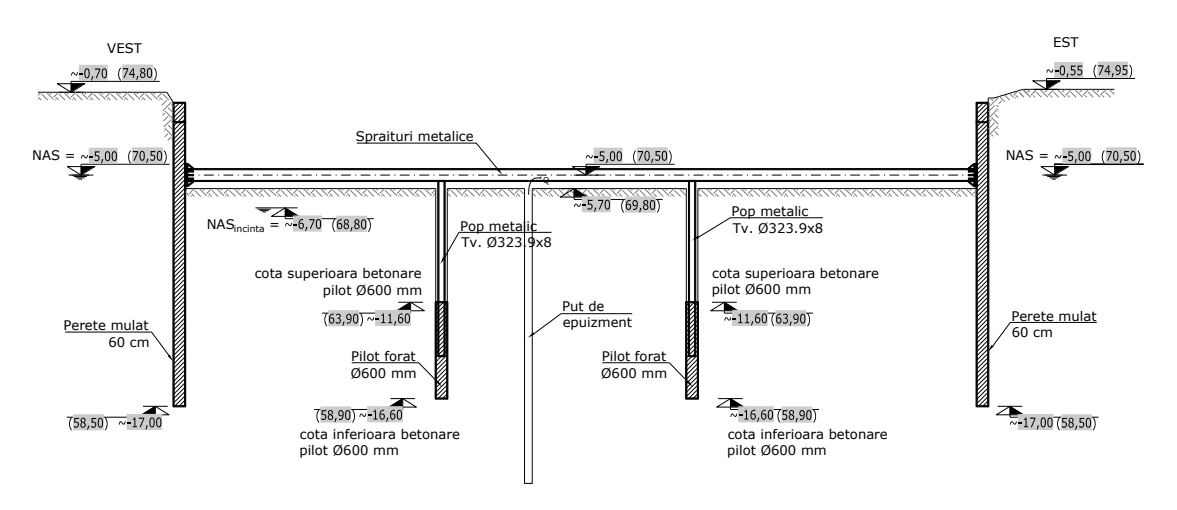


Figure IV.3 - Stage 2 - Excavation down to elevation -5.70 and installation horizontal strut at elevation -5.00

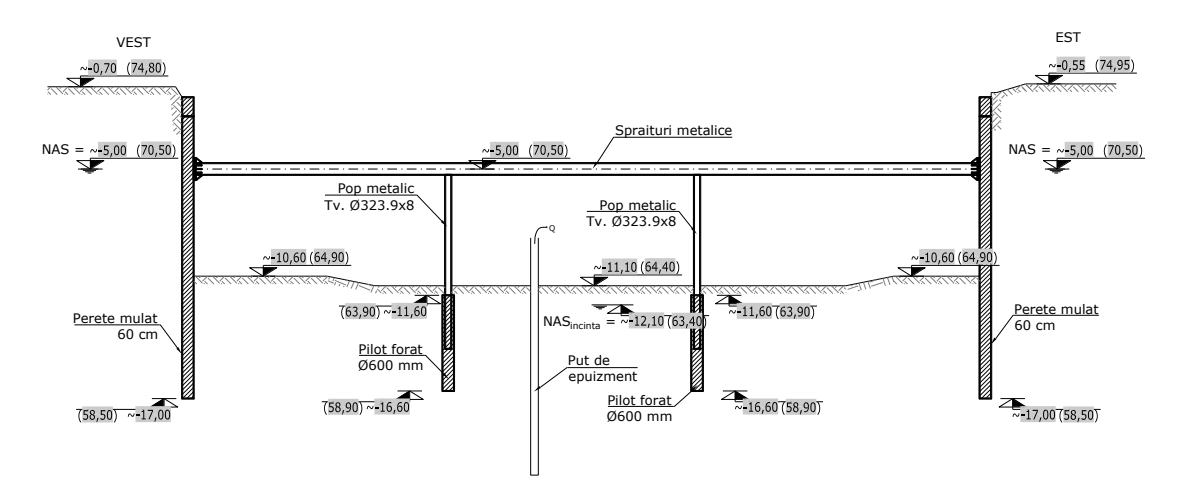


Figure IV.4 - Stage 3 - Excavation down to -11,10

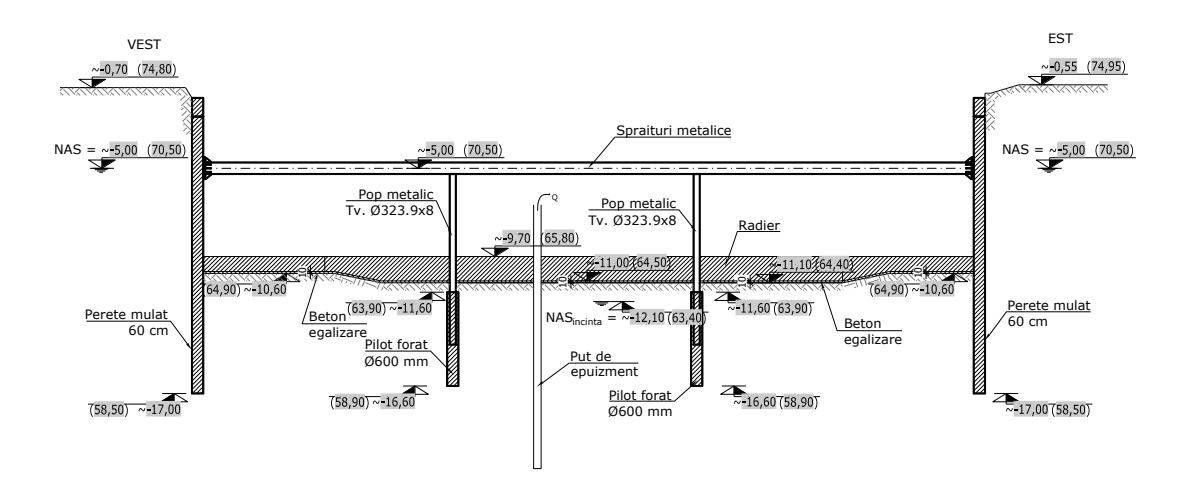


Figure IV.5 - Stage 4 - Raft construction

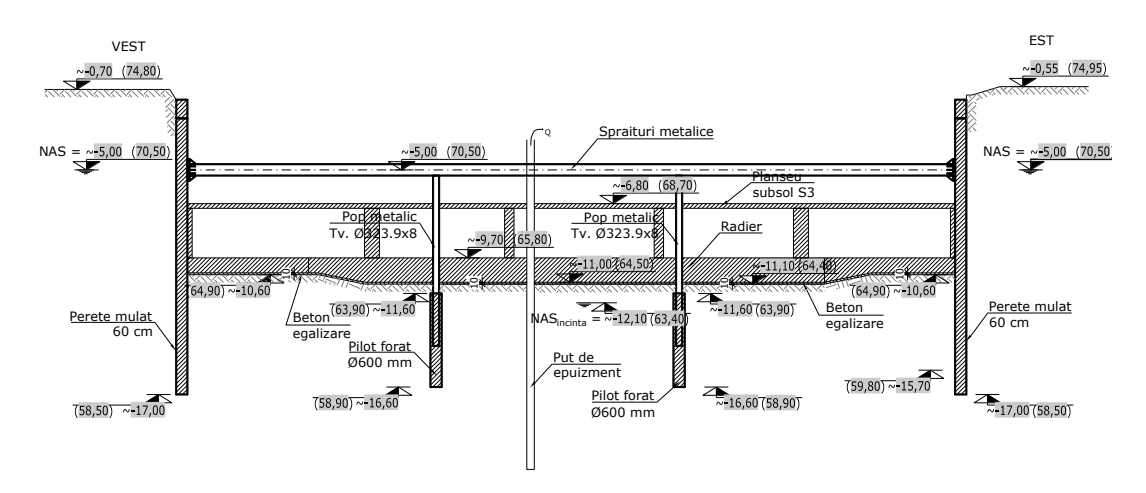


Figure IV.6 - Stage 5 - Execution of basement S3.

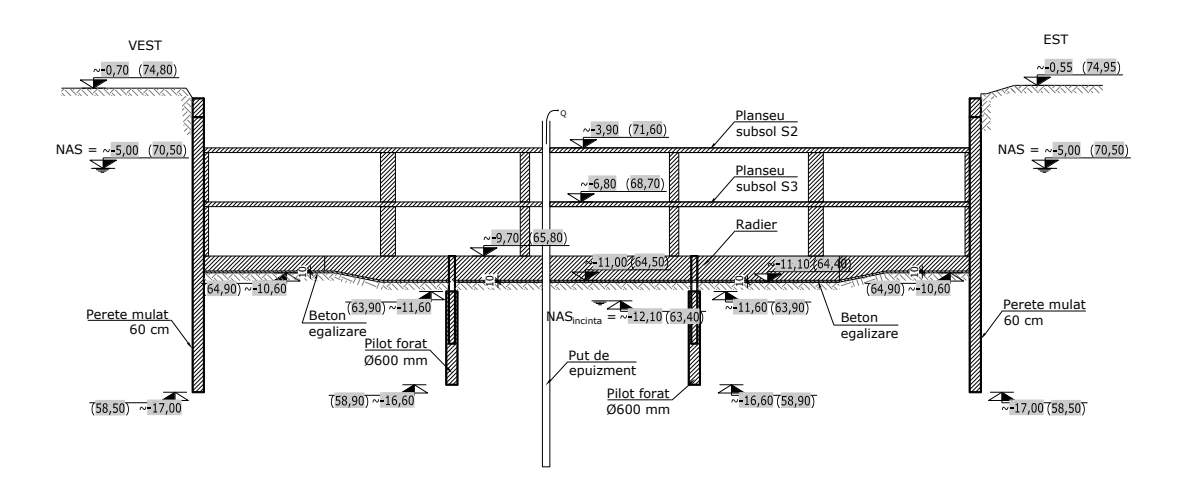


Figure IV.7 - Stage 6 - Dismantling of the metal struts at elevation - 5,00 and execution of basement S2

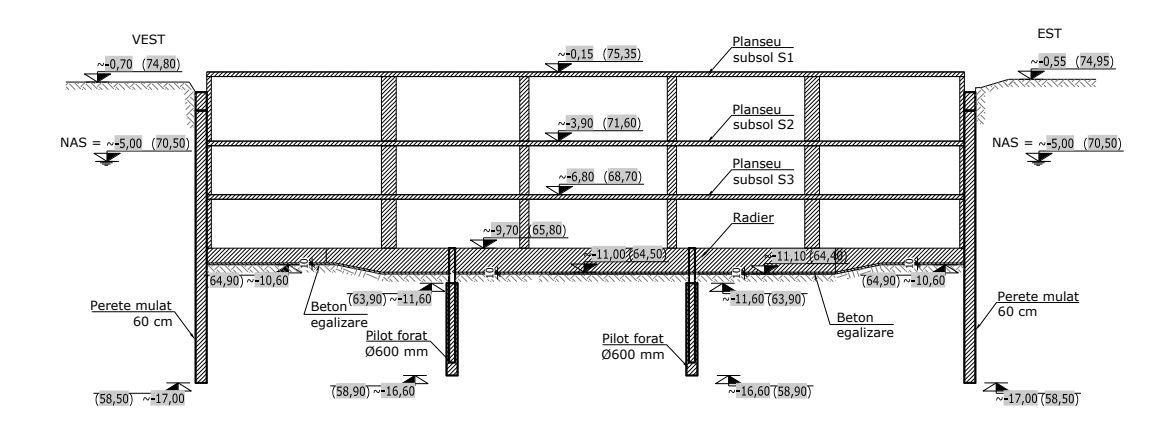


Figure IV.8 - Stage 7 - Execution of basement S1 and floor slab  $\pm 0,00$ 

# IV.4.1 Results of soil-structure interaction analysis

The analysis of soil-structure interaction results involves the calculation and verification of displacements, deformations and stresses in foundation elements and in the soil.

The evaluation of the soil-structure interaction was done in the plane state of deformation, using the numerical finite element method using the PLAXIS 2D 2019.00 software.

The PLAXIS 2D 2019.00 program is suitable for numerical analysis of supporting and foundation systems in particular due to the availability of advanced constitutive models used in modelling the non-linear behavior of soils. This is particularly important for modelling as realistically as possible the interaction between soil and structure. Another advantage of this software is the possibility of step-by-step calculation, which ensures a realistic simulation of the construction.

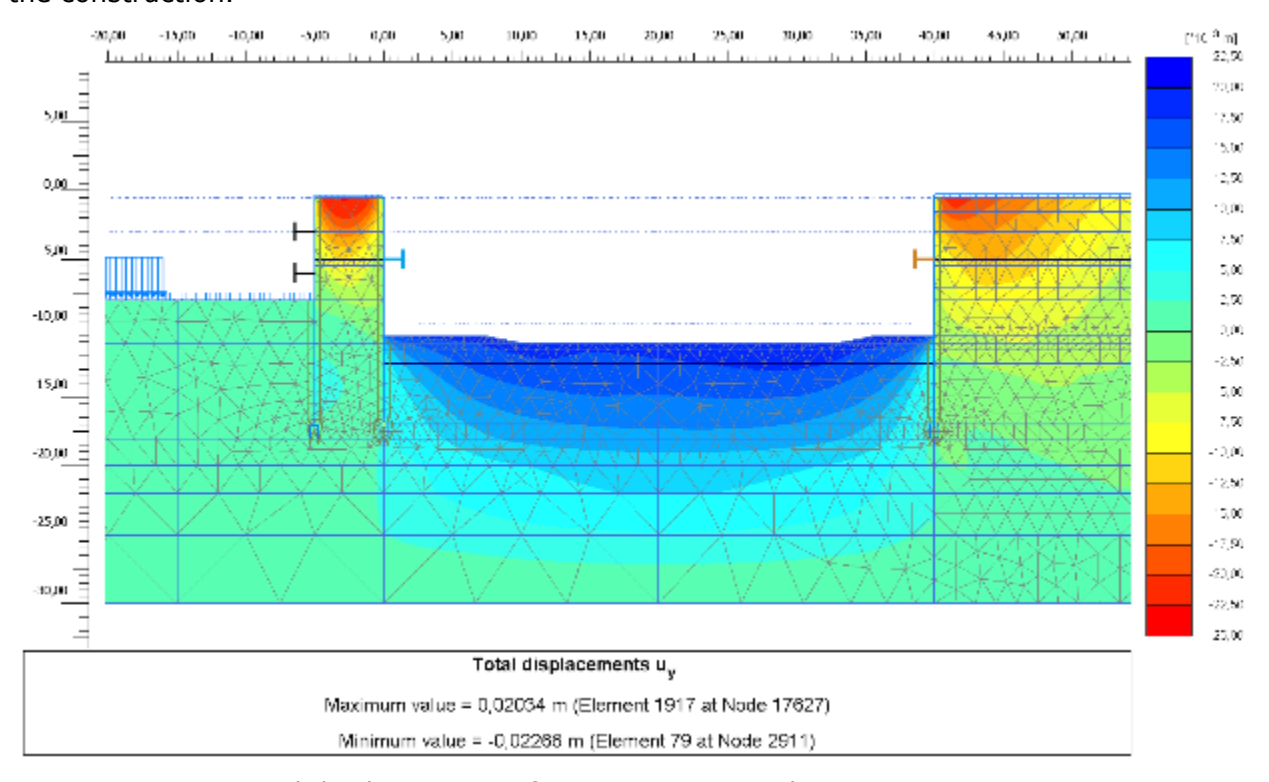


Figure IV.9 - Vertical displacements after excavation at elevation -11,10

The results of the calculation in Plaxis 2D 2019.00, shown in Figure IV.9, reveal a vertical deformation of the ground after excavation up to elevation -11.10, mainly due to its decompression/heaving. The vertical deformation has a value of ca.  $\sim$ 2.3 cm (heaving effect or heaving of the base of the excavation).

According to the geotechnical investigations carried out on the site, the excavation ends in layer 4, "Colentina sands and gravels".

Figure IV.10 shows the results of the calculation in terms of vertical ground deformations under the foundation system under the long-term loading obtained from the numerical analysis.

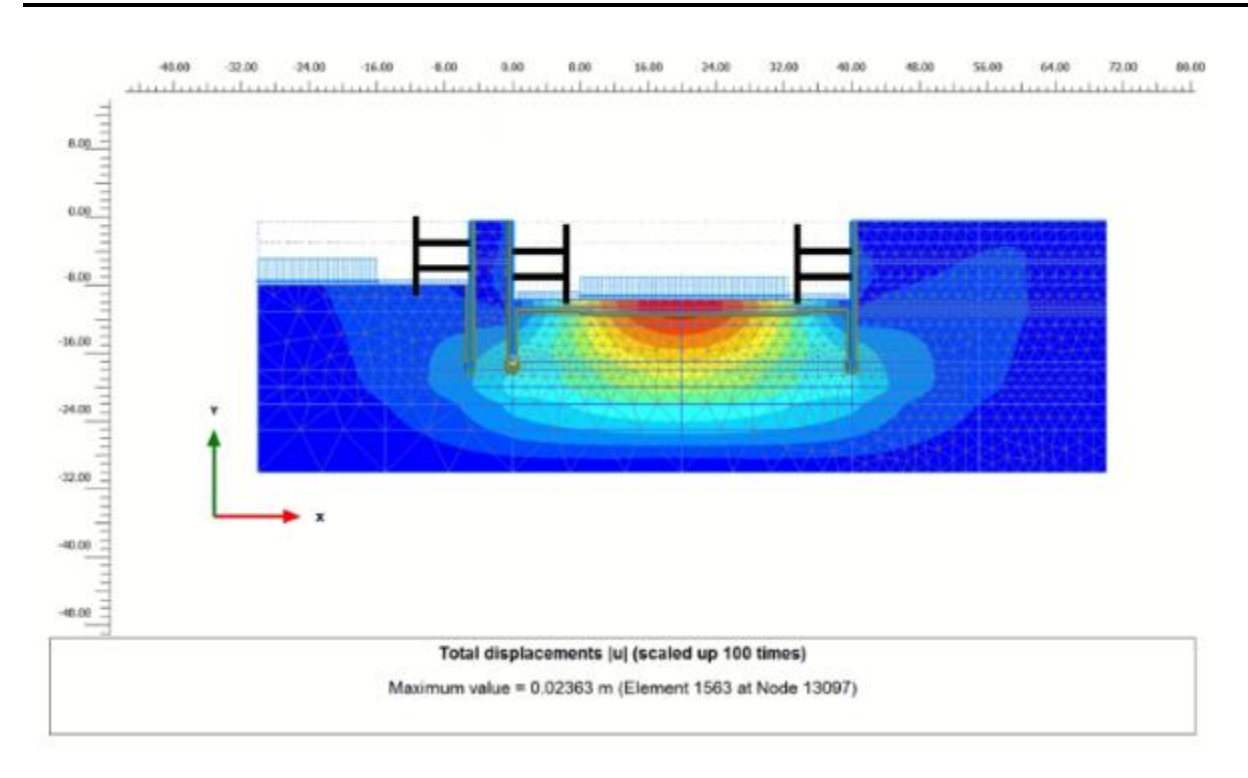


Figure IV.10 - Total displacements under long-term loads

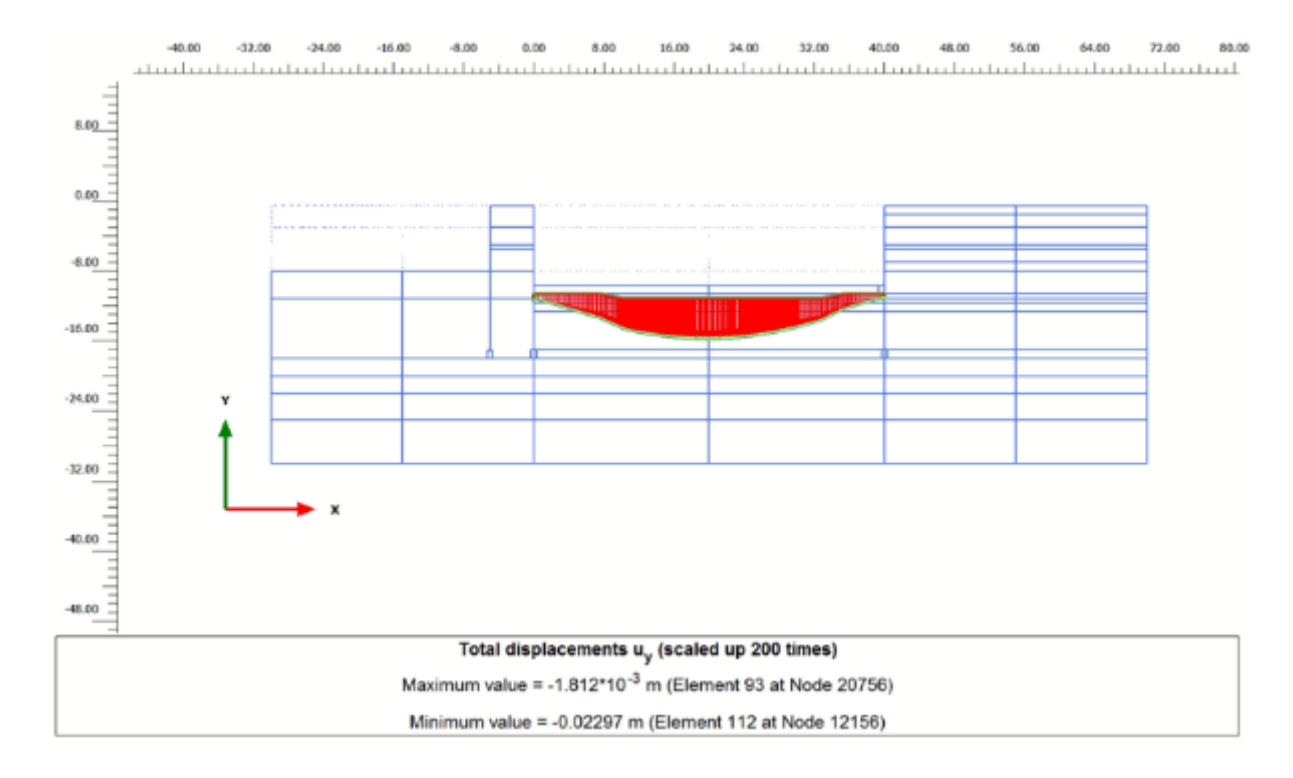


Figure IV.11 - Foundation settlements under long term loading,  $s_{max} = \sim 2.2~cm$ 

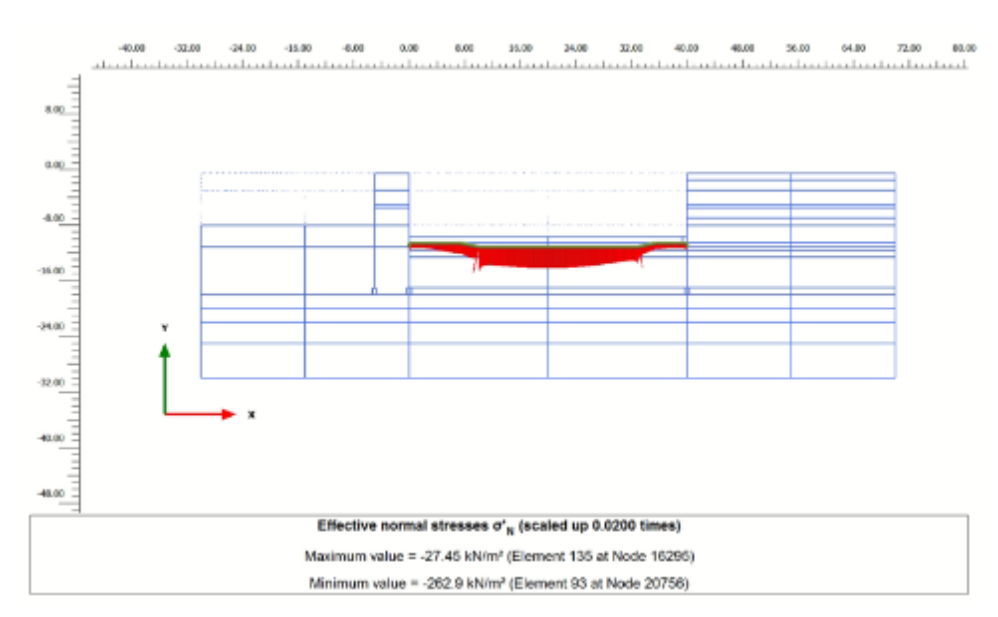


Figure IV.12 - Effective pressure transmitted to the ground by the general embankment

Figures IV.11 and IV12 show the deformation, i.e., the pressure on the soil, under long term loads from the superstructure. As can be seen from the figures, a maximum settlement of 2.2 cm, the maximum pressure transmitted to the soil is about 263 kPa.

Given the large dimensions of the deep excavation, the geometry and the large number of structural elements, as well as the need to use non-linear constitutive laws for modelling the behavior of the soil, the soil structure interaction was analyzed in detail by means of representative sections in plane state deformations. The interaction analysis was performed for static conditions.

#### Section S1-1 calculation:

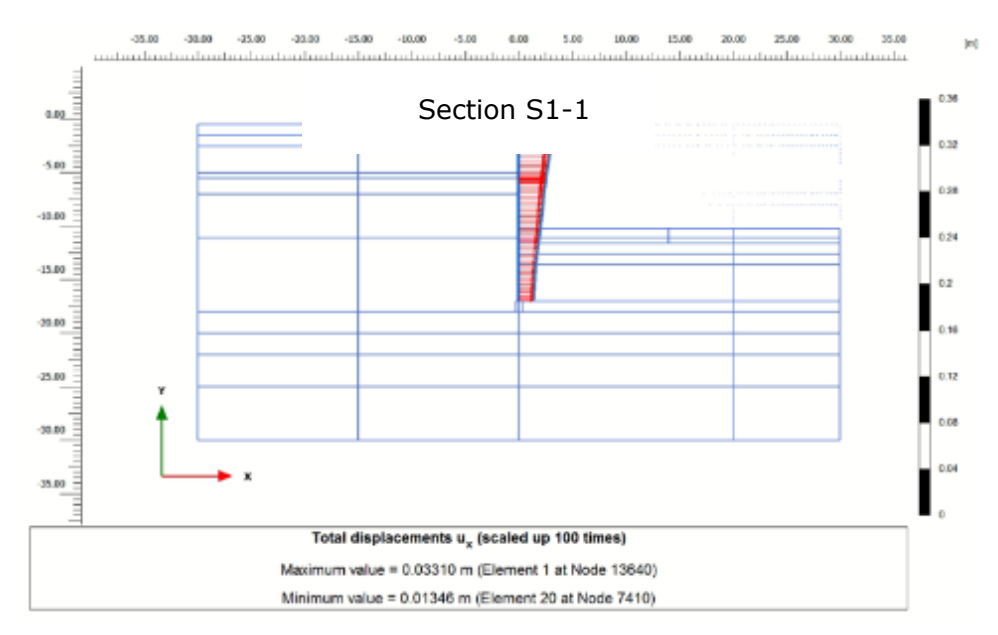


Figure IV.13 - Horizontal displacement of the diaphragm wall - Section S1-1, during the casting of the slab over the basement S2  $\,$ 

Figure IV.13 shows the diagram of the horizontal displacement at the design section S1-1 during the casting of the floor slab over the basement S2. The maximum calculated horizontal displacement is 33 mm.

### IV.5 Geotechnical Monitoring

This chapter presents the main monitoring equipment installed for monitoring during construction and during operation of the new structure. Figure IV.14 show the monitoring equipment installed.

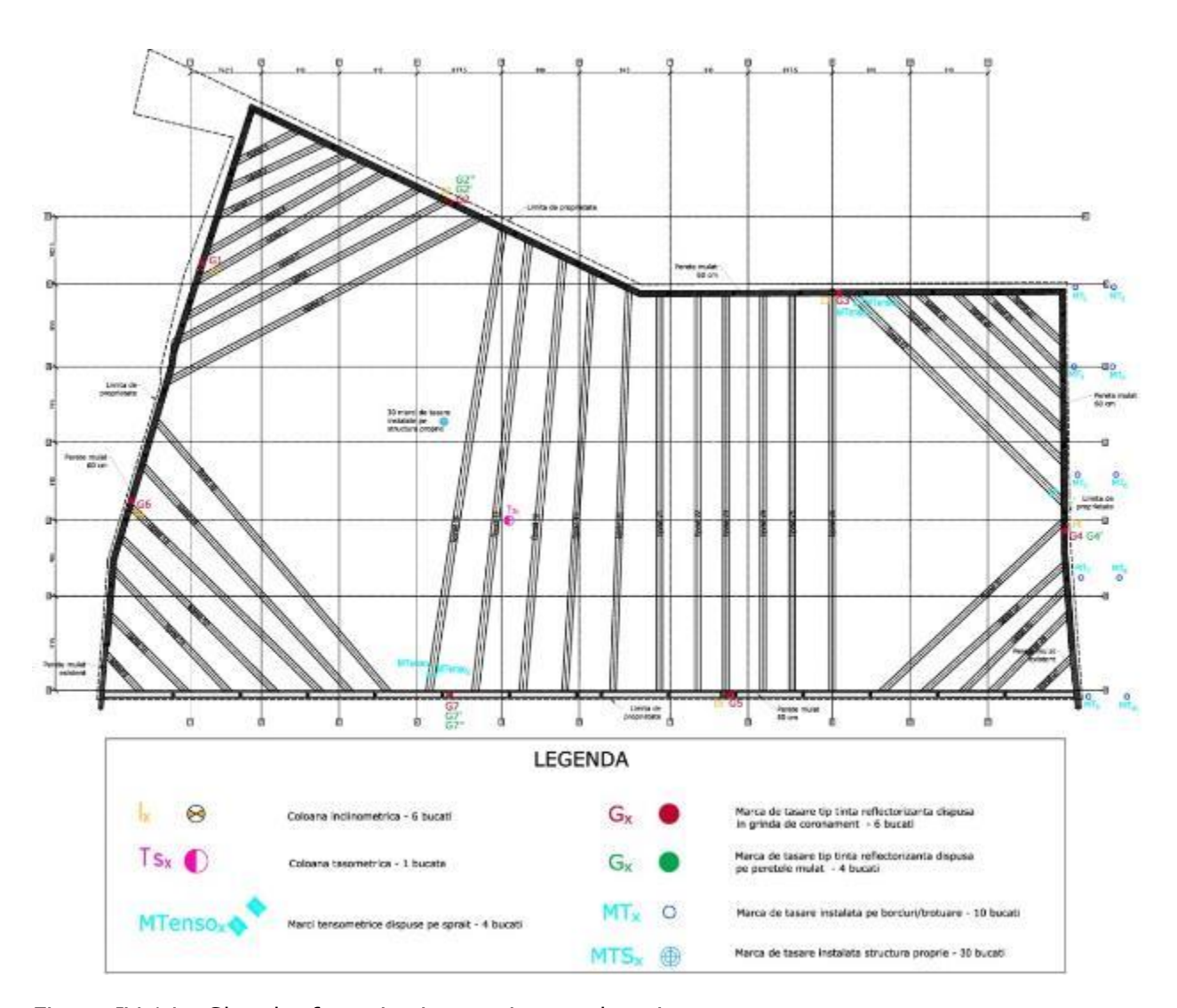


Figure IV.14 - Sketch of monitoring equipment location

### IV.6 Geotechnical monitoring results

In order to be able to make an assessment of the parameters used in the modelling of the structure, previously presented, the data obtained from the geotechnical monitoring were used. Analyzing the data provided by the geotechnical monitoring, we can observe the difference between the modelled situation and the real behavior of the foundation ground.

# IV.6.1 Monitoring results using inclinometer

The figures below show the results of the inclinometer monitoring. Figures IV.15 and IV.16 show the situation of inclinometer I1, specific to geotechnical monitoring, and the situation of the section near inclinometer I1, specific to geotechnical modelling using the Mohr-Coulomb model. Thus, we can observe a measured displacement of about 17 mm compared to a modelled displacement of about 19 mm.

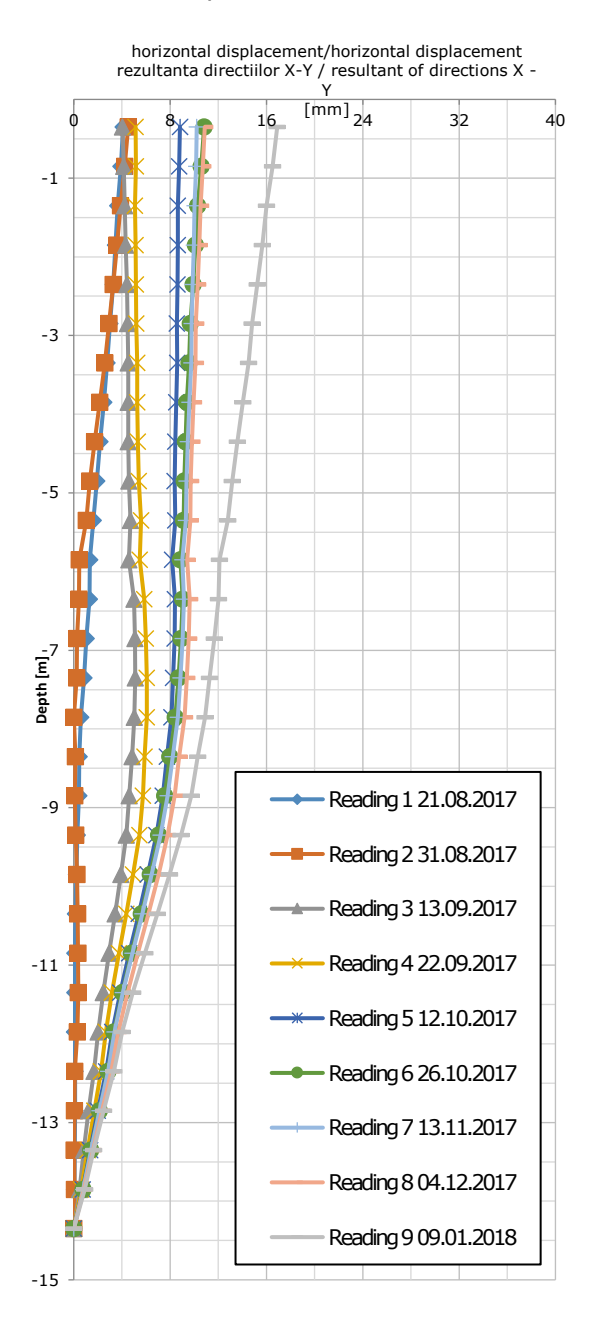


Figure IV.15 - Horizontal displacement measured in inclinometer column  $I_1$  (maximum 17 mm)

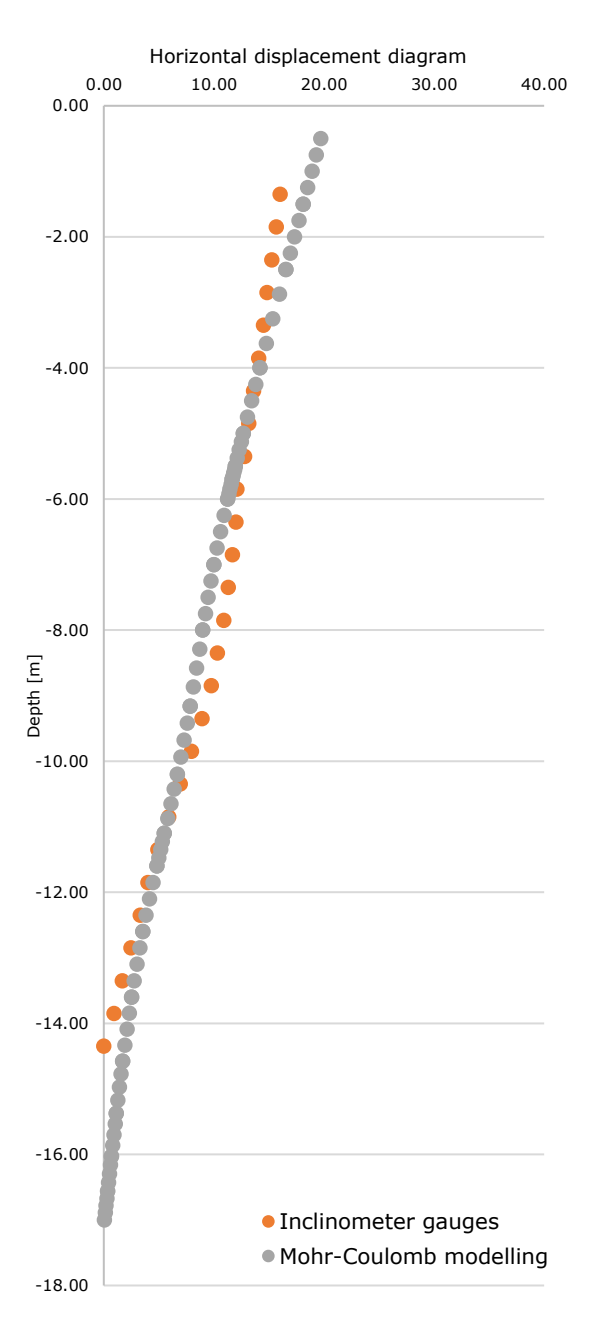


Figure IV.16 - Comparison diagram between the values resulting from the inclinometer measurements and those resulting from the modelling in Plaxis 2D

#### IV.7 Geotechnical model validation and calibration

### IV.7.1 Validation of the numerical model

Validation refers to the degree of accuracy with which a numerical model approximates the real physical phenomenon. In order to be able to use a result obtained by numerical modelling, it needs to be properly validated. Validation of the numerical model ensures that the main aspects characterizing the physical phenomenon are included and that the results provided are plausible and representative of the real situation.

In the process of modelling the real physical phenomenon the following steps can be identified below.

The first step in the modelling process is to simplify the real phenomenon by applying simplifying assumptions and retaining only those elements that are essential to the process under study. This results in a simplified model of the real phenomenon, which is then used to translate it into a mathematical model.

The mathematical model is characterized by the set of equilibrium equations, the boundary conditions and the constitutive model describing the behavior of the soil in the studied phenomenon. The transition from the mathematical to the numerical model requires the model to be discretized by implementing it in specialized software.

The choice of a constitutive model should be based on an assessment of the model's ability to describe the essential aspects of the soil's behavior within the phenomenon under study. Thus, the constitutive model provides a qualitative description of the behavior of the soils, while the geotechnical parameters are intended to quantify this behavior (Brinkgrieve, 2013).

Before analyzing the numerical model as a whole, the component parts have to be validated, here referring to the evaluation of the behavior of the constitutive model in laboratory tests. There are now many computer programs that facilitate this verification by including modules that simulate the usual laboratory tests.

In situ measurements of the phenomenon under study thus become particularly important in the validation process, especially for complex phenomena. Data obtained in the field allow a comparative analysis with numerical model results and calibration of computational models.

#### IV.7.2 Calibration of the calculation model

The choice of this model to simulate the behavior of the soil in its natural state is justified by its particularity compared to elasto-plastic models to capture the non-linearity of the stress-strain relationship, the stiffness as a function of the stress level and the inelastic behavior of the soil.

The choice of the initial set of parameters is based on the results of the in-situ and laboratory tests carried out as part of the geotechnical study. The parameters were then calibrated so as to obtain a satisfactory correlation between the displacement or subsidence profile over the depth or width of the structural element and that measured in-situ.

## IV.7.3 Calibration of geotechnical parameters

This subchapter will present how the calibration of geotechnical parameters was performed. As a first input point, the values of geotechnical parameters determined by correlations presented in Research Report 2 were used.

The geotechnical model was developed using a program using the finite element method, called Plaxis2D. Two models were used to calibrate the geotechnical parameters using the Mohr-Coulomb model as a constitutive model.

The first model, generically referred to as "Model 1", was a simulation of the interaction of the new structure with the bedrock in terms of subsidence calculation using as loading level, the loads evaluated for the long-term loading situation. This model was helpful in calibrating mainly parameters such as deformation moduli below the foundation elevation. Calibration was performed using data from monitoring of displacement with a strain gauge type device. There were several iterations in which the parameters were adjusted so that the two curves representing the settlement at depth were as close as possible.

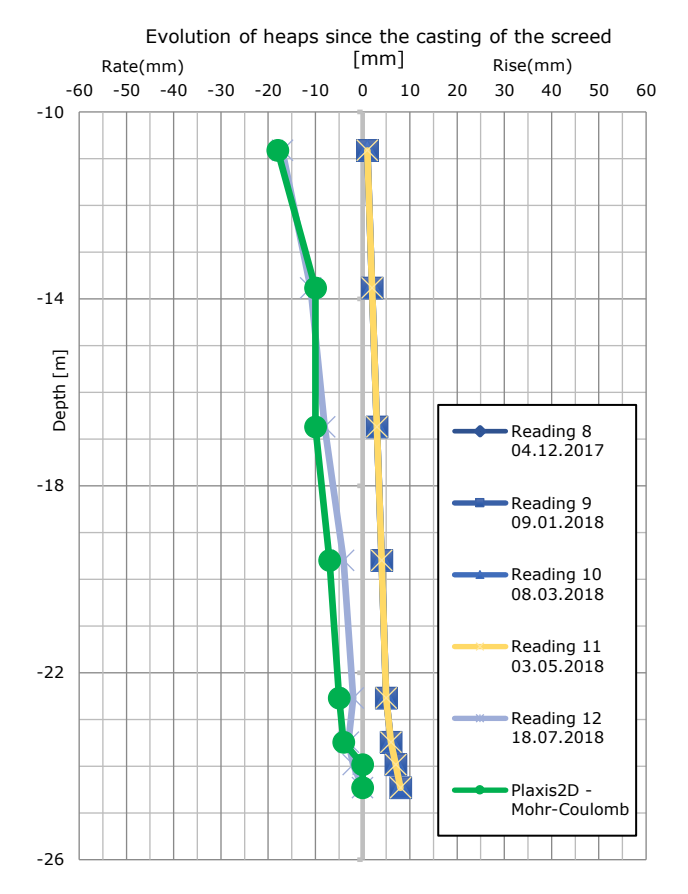


Figure IV.17 - Horizontal displacement measured in inclinometer column  $I_1$  (maximum 17 mm)

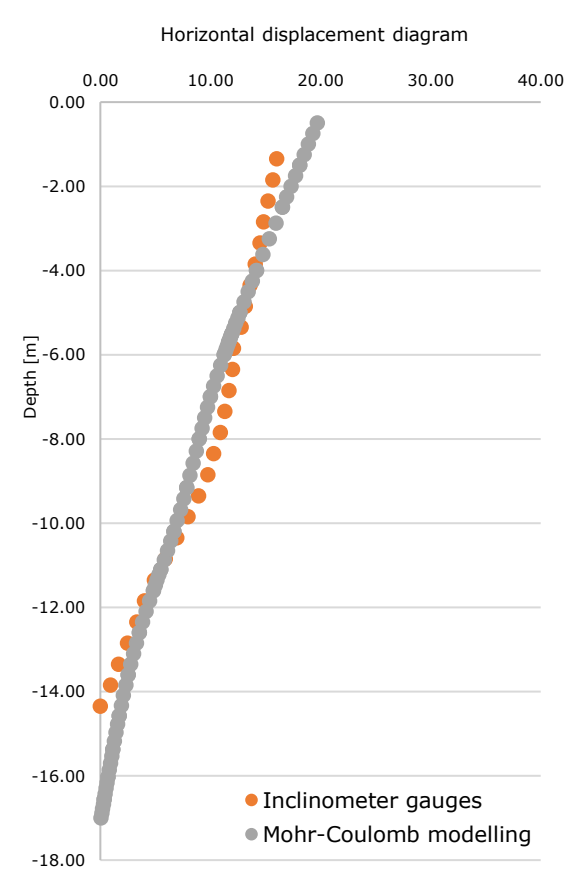


Figure IV.18 - Comparison diagram between the values resulting from the inclinometric measurements and those resulting from the modelling in Plaxis 2D

The second model, "Model 2" represented the modelling of the behavior of a diaphragm wall corresponding to section S1-1. Section 1-1 was monitored, during the execution of the works, using an inclinometer column. Using as input the parameters determined according to

the correlations presented in Research Report No. 2 and the deformation moduli calibrated using "Model 1". Model 2 aimed at calibrating mainly the shear parameters and a fine tuning of the geotechnical parameters describing how a soil behaves when subjected to deformation. The graph is shown in Figure IV-18.

Using the procedure described above, the following geotechnical parameters specific to the Mohr-Coulomb model were obtained.

Table IV.2. Values of geotechnical parameters considered, calibrated for the Mohr-Coulomb model

Coloulation laves	Relative elevation	η	E′	φ'	c'	٧
Calculation layer	±0,00	[kN/m ] <sup>3</sup>	[ MN/m ] <sup>2</sup>	[°]	[kN/m ] <sup>2</sup>	-
1. Filling	-0,50 ÷ -1,50	18	10	20	50	0.35
2. Sandy complex	-1,50 ÷ -5,00	18	12	30	5	0.30
3. Clayey lens	-5,00 ÷ -7,00	18	7	18	45	0.38
4. Colentina sands and gravels	-7,00 ÷ -11,10	18	30	30	5	0.30
5. Intermediate clay complex	-11,10 ÷ -18,00	18	20	16	115	0.40
6. Mostistea sands	-18,00 ÷ -20,00	19	120	42	1	0.28
7. Clay	-20,00 ÷ -22,00	18	40	15	115	0.40
8. Mostistea sand	sub -22,00	19	90	42	1	0.28

### IV.7.4 Interpretation of results

The table below summarizes the correlations and parameters resulting from the calculations in Research Report 2 and the parameters calibrated according to the procedures outlined in the previous sub-chapter.

Table IV.3 - Comparison of the initially determined parameter values and the calibrated parameter values for the Mohr-Coulomb model according to Research Report 3

Source Correlation	Correlation according to Research Report 2	Value cf. 2	Calibrated value	Correlated correlation for the Mohr-Coulomb model
LB own correlation	$tan\phi = 0.1q_c + 0.1$	0,231 (13°)	0,487 (26°)	$tan\phi' = 0.2 - q_c + 0.1$
LB own correlation	$Cu = 0.04 \times qc - 0.01$	42 kPa	65 kPa	$c' = 0.05 - q_c$
LB own correlation	Eoed2-3 = $3,1qc + 3$	7.100 kPa	7.000 kPa	$E_{50} = 3.1 - q_c + 3$
NPC own correlation	$tan\phi = 0.003 \times qc + 0.67$	0,719 (36°)	(0,624) 32°	tanφ' = 0.035 - q <sub>c</sub>
NPC own correlation	$M_{DMT} = 5.1 \times qc - 8$	75,000 kPa	30.000 kPa	$E' = 3 - q_c - 8$
Own correlation CAI	$tan\phi = 0.1q_c + 0.01$	0,277 (16°)	0,267 (15°)	tanφ' = 0,1 - q <sub>c</sub>
Own correlation CAI	$Cu = 0.045 \times qc + 0.02$	140 kPa	115 kPa	$c' = 0.045 - q_c$
Own correlation CAI	$MDMT = 11.5 \times qc - 2$	28,000 kPa	15,000 kPa	$E' = 7 - q_c - 2$

After the realization and calibration of the parameters for the two Mohr-Coulomb models mentioned above, iterative- calculations were performed, keeping the model but changing the

constitutive models. Parameter calculations and calibrations were performed for both the Hardening-Soil and the Hardening Soil with Small Strains models.

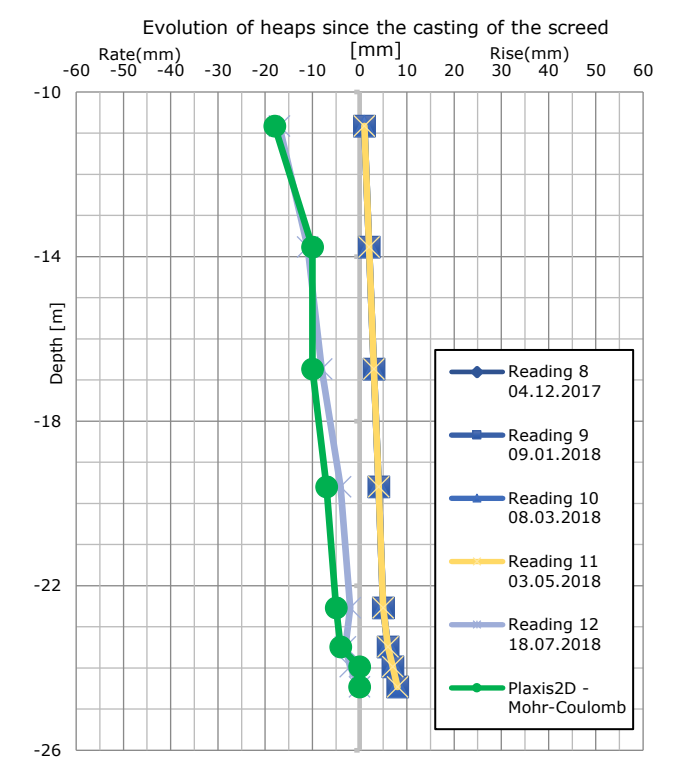


Figure IV.18 - Horizontal displacement measured in inclinometer column  $I_1$  (maximum 17 mm)

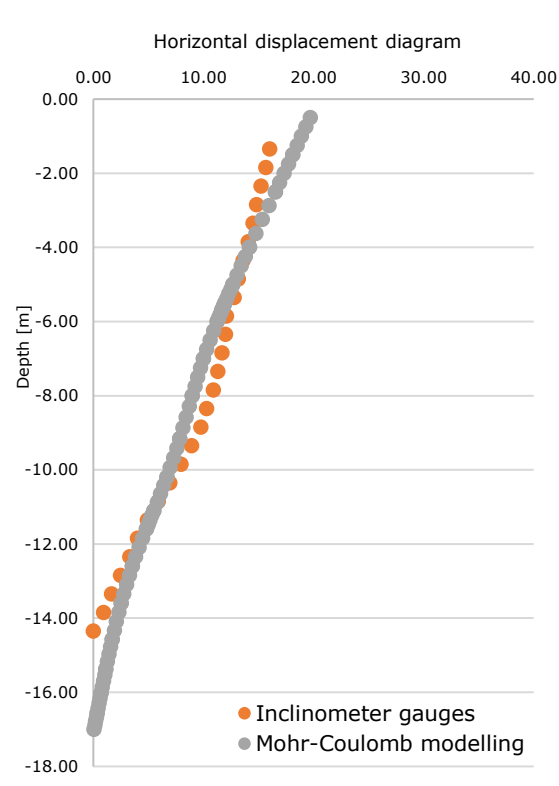


Figure IV.19 - Comparison diagram between the values resulting from the inclinometric measurements and those resulting from the modelling in Plaxis 2D

Table IV.4. Values of geotechnical parameters considered, calibrated for the Hardening-Soil model

Coloulation lavor	Relative elevation	γ	E <sub>50</sub>	Eur	□'	c'
Calculation layer	±0,00	kPa	MPa	MPa	0	kPa
1. Filling	-0,50 ÷ -1,50	18	8	40	25	50
2. Sandy complex	-1,50 ÷ -5,00	18	18	70	34	5
3. Clay lens	-5,00 ÷ -7,00	18	10	50	20	60
4. Colentina sands and gravels	-7,00 ÷ -11,10	18	40	120	36	5
5. Intermediate clay complex	-11,10 ÷ -18,00	18	25	125	15	125
6. Mostistea sands	-18,00 ÷ -20,00	19	50	160	42	5
7. Clay	-20,00 ÷ -22,00	18	20	100	15	115
8. Mostistea sand	sub -22,00	19	40	160	42	5

Table IV.5 - Comparison of initial determined parameter values and calibrated parameter values for the Hardening Soil model according to Research Report No. 3

Source Correlation	Correlation according to Research Report 2	Value cf. 2	Calibrated value	Correlated correlation for the Mohr-Coulomb model
Own correlation LB	$tan\phi = 0.1q_c + 0.1$	0,231 (13°)	0,363 (20°)	$tan\phi' = 0.2 - q_c + 0.1$
Own correlation LB	$Cu = 0.04 \times qc - 0.01$	42 kPa	70 kPa	$c' = 0,055 - q_c$
Own correlation LB	Eoed2-3 = $3,1qc + 3$	7.100 kPa	10,000 kPa	$E_{50} = 5.3 - q_c + 3$
NPC own correlation	$tan\phi = 0.003 \times qc + 0.67$	0,719 (36°)	(0,719) 36°	$tan\phi' = 0.015 - q_c + 0.5$
NPC own correlation	$M_{DMT} = 5.1 \times qc - 8$	75,000 kPa	40,000 kPa	$E_{50} = 2.2 - q_c - 5$
Own correlation CAI	$tan\phi = 0.1q_c + 0.01$	0,277 (16°)	0,267 (15°)	$tan\phi' = 0.1 - q_c - 0.01$
Own correlation CAI	$Cu = 0.045 \times qc + 0.02$	140 kPa	125 kPa	$c' = 0.047 - q_c$
Own correlation CAI	$MDMT = 11.5 \times qc - 2$	28,000 kPa	25,000 kPa	$E_{50} = 9 - q_c - 2$

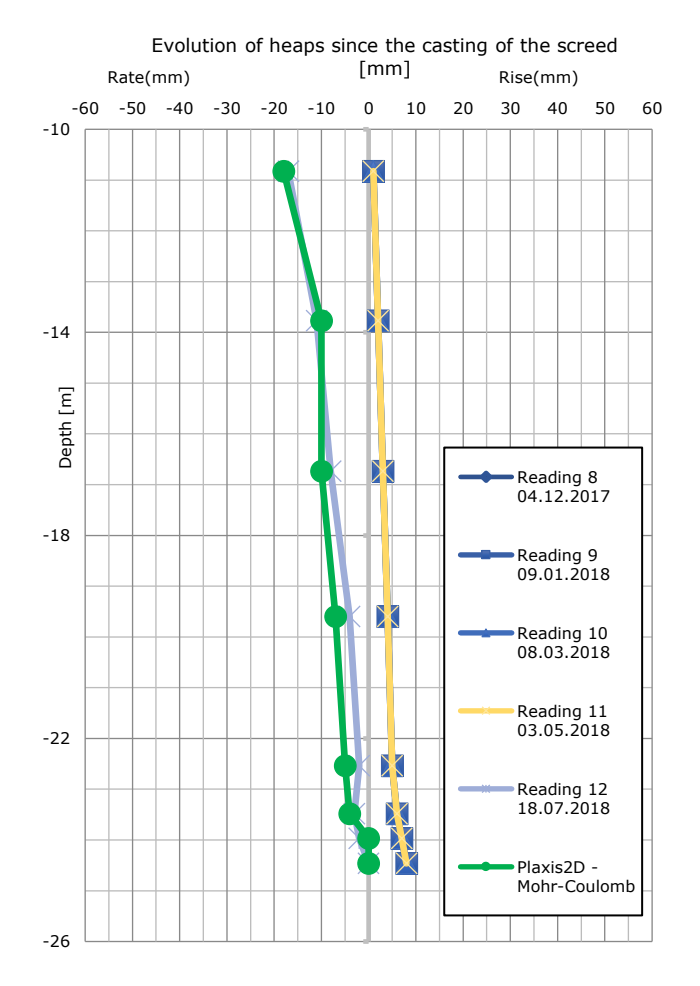


Figure IV.18 - Horizontal displacement measured in inclinometer column  $I_1$  (maximum 17 mm)

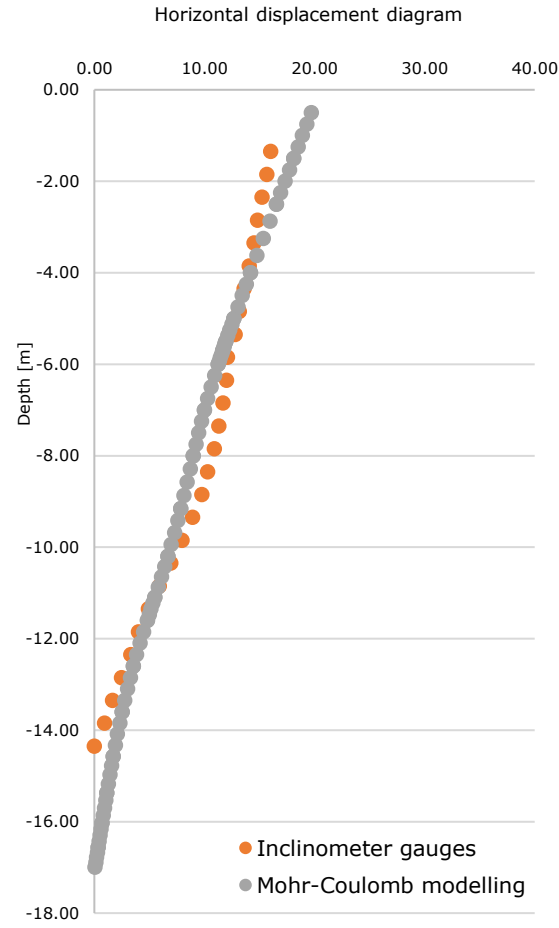


Figure IV.19 - Comparison diagram between the values resulting from the inclinometer measurements and those resulting from the modelling in Plaxis 2D

Table IV.6. Values of the considered geotechnical parameters calibrated for the Hardening-Soil model

Calaudatian lawan	Relative	γ	E <sub>50</sub>	Eur	□'	c'	G <sub>0</sub>
Calculation layer	elevation $\pm 0,00$	kPa	MPa	MPa	0	kPa	MPa
1. Filling	-0,50 ÷ -1,50	18	6	24	25	50	40
2. Sandy complex	-1,50 ÷ -5,00	18	12	48	30	5	35
3. Clay lens	-5,00 ÷ -7,00	18	7	30	18	45	30
4. Colentina sands and gravels	-7,00 ÷ -11,10	18	30	90	32	2	70
5. Intermediate clay complex	-11,10 ÷ -18,00	18	15	60	16	115	100
6. Mostistea sands	-18,00 ÷ -20,00	19	40	120	40	5	200
7. Clay	-20,00 ÷ -22,00	18	30	150	15	115	180
8. Mostistea sand	sub -22,00	19	40	120	40	5	200

Table IV.7 - Comparison of initial determined parameter values and calibrated parameter values for the Hardening Soil model according to Research Report No. 3

Source Correlation	Correlation according to Research Report 2	Value cf. 2	Calibrated value	Correlated correlation for the Mohr-Coulomb model
Own correlation LB	$tan\phi = 0.1q_c + 0.1$	0,231 (13°)	0,325 (18°)	$tan\phi' = 0.17 - q_c + 0.1$
Own correlation LB	$Cu = 0.04 \times qc - 0.01$	42 kPa	45 kPa	$c' = 0.035 - q_c$
Own correlation LB	Eoed2-3 = $3,1qc + 3$	7.100 kPa	7.000 kPa	$E_{50} = 3.1 - q_c + 3$
NPC own correlation	$tan\phi = 0.003 \times qc + 0.67$	0,719 (36°)	(0,624) 32°	$tan\phi' = 0.013 - q_c + 0.4$
NPC own correlation	$M_{DMT} = 5.1 \times qc - 8$	75,000 kPa	30.000 kPa	$E_{50} = 2 - q_c - 3$
Own correlation CAI	$tan\phi = 0.1q_c + 0.01$	0,277 (16°)	0,277 (16°)	tanφ' = 0,1 - q <sub>c</sub>
Own correlation CAI	$Cu = 0.045 \times qc + 0.02$	140 kPa	115 kPa	$c' = 0.045 - q_c$
Own correlation CAI	$MDMT = 11.5 \times qc - 2$	28,000 kPa	15,000 kPa	$E_{50} = 9 - q_c - 2$



## V Conclusions and perspectives

This report presents the correlation calibrations of the parameters obtained in Research Report 2.

The first chapter is a brief introduction to the subject of the report and details of the objectives. The assessment of correlations between different geotechnical parameters was carried out for three lithological layers. Starting from surface to depth, the layers, commonly referred to as "Bucharest Loam", "Colentina Sands and Gravels" and "Intermediate Clay Complex" were analyzed. These layers were chosen as they significantly influence most geotechnical works, such as direct foundations, deep foundations, support works and tunnels.

Modelling was carried out to simulate soil behavior using three constitutive models, Mohr-Coulomb, Hardening Soil and Hardening Soil with small strain stiffness. Data from geotechnical monitoring of the layers during and after completion of the construction were used for correlation checking and back-calculation. The instruments used for the monitoring of the structures presented in this report were inclinometers, extensometers and tilt marks (geometric levelling).

The second chapter briefly presents the above-mentioned monitoring tools, the underlying technology and the monitoring results.

Chapter 3 details the common constitutive models used in geotechnical engineering. Also, in this chapter the main parameters underlying these models are presented, as well as the advantages and disadvantages of each constitutive model. Constitutive models are essential in modelling the behavior of soils for current geotechnical design. Over time, numerous models have been developed, from the simplest to the most complex. These are based on complex equations that attempt to describe the behavior of the soil as faithfully as possible. The choice of a particular model for the design of a geotechnical structure has to be made with great care as the more complex models do not necessarily give more realistic results and user experience becomes important. For the use of more complex models, parameters are needed, which are obtained from more laborious and operator sensitive tests.

Chapter 4 presents in detail the models that were the basis for the correlations. The results of the monitoring and their interpretation are also presented. Back calculations were performed using these data. These back calculations were necessary to calibrate the calculation models and the resulting curves and graphs with the monitoring results.

It should be noted that following the calculations presented in Chapter 4 the correlations for the Mohr-Coulomb, Hardening Soil and Hardening Soil with small strain stiffness constitutive models were determined.

It should be noted that the results using advanced constitutive models show values very close to those obtained directly from the field. Thus, while for HS-Small the values obtained were similar to those obtained from laboratory and in situ investigations, using the Mohr-Coulomb model the parameter values are generally higher. This implies, theoretically, that if the Mohr-Coulomb constitutive model is used in the design, higher values can be used to obtain the same subsidence or lateral displacements.

Further checks/validations are planned to be carried out within the thesis to assess the correlations determined. In practice, structures will be dimensioned using advanced numerical methods (FEM), which will be compared with the data provided by the geotechnical monitoring

of the respective works, collected during the construction of the structures and after their completion. This analysis involves performing a back-calculation to validate the calculation model. On the basis of the results obtained, useful conclusions can be drawn on the validity of the correlations used and, if necessary, the correlations will be corrected.

### VI Bibliography

ASTM D-1586 - 11, Standard Test Method for Standard Penetration Test (SPT) and Split-Barrel Sampling of Soils.

ASTM D-6635 - 01, 2007. Standard Test Method for Performing the Flat Plate Dilatometer.

ASTM D6951 - 03, 2015. Standard Test Method for Use of the Dynamic Cone Penetrometer in Shallow Pavement Applications.

Akinson, J., D. Farrar Stress Path Tests to Measure Soils Strength Parameters for Shallow Landslips, In: Proc. XI ICSMFE, San Francisco, volume 2, 983 - 986, Rotterdam, A. A. Balkema, 1985.

Atkinson, A., 2010. Mechanics of soils.

Bauer, E. Calibration of a Comprehensive Hypoplastic Model for Granular Materials. Soils and Foundations, 36 (1996), No. 1, 13-26.

Biedermann, 1984. Vergleichende Untersuchungen mit Sondeen in Schluff" Forschungsberichte aus Boden-mechanik und Grundbau.

Brinkrieve, R.B.J et al, *Plaxis 3D User's manuals*, Delft University of Technology, Delft, Nederlands, 2015

BS5930:1999, 1999. Code of practice for site investigations for higher education. London: British Standards Institution.

Butcher et al., 1995. Determining the modulus of the ground from in situ geophysical testing. Hamburg,

C159-89, 1989. Technical instructions for investigation of bedrock by cone penetration method, static penetration, dynamic penetration, vibropenetration. Bucharest: s.n.

Cassn M, 1988. In situ tests in soil mechanics, Realization and Interpretation. Volumul 1, pp. 146-151.

Cambou, B., C. Di Prisco (Eds). Constitutive Modelling of Geomaterials, Hermes, 2000.

Capraru, C. Studies on the calculation of the enclosures of large deep excavations, PhD Thesis, Technical University of Construction, Bucharest, Romania, 2012

D-5778, A., 2006. Standard Test Method for Performing Electronic Friction Cone and Piezocone Penetration Testing of Soils.

DeBeer, 1967. Proefondervindelijke Bijdrage tot de studie van zand onder funderingem opstaal.

DIN 1054:2010-12, 2012. Baugrund - Sicherheitsnachweise im Erd- und Grundbau - Ergänzende Regelungen zu. Berlin: Deutsches Institut für Normung.

DIN 4094-3:2002, 2002. Baugrund - Felduntersuchungen - Teil 3: Rammsondierungen. Berlin: Deutsches Institut für Normung.

Duncan, J. M., C.-Y. Chang. Nonlinear Analysis of Stress and Strain in Soils Journal of the Soil Mechanics and Foundations Division ASCE, 96 (1970), No. SM5, 16291653-, 1970

Eurocode 7, 1997. Geotechnical design - Part 3: Design assisted by field testing, Section 9: Flat dilatometer test.

Finno, 1993. Analytical interpretation of dilatometer penetration though saturated cohesive soils. Geotechnique, 43(2), pp. 241-254.

Gudehus, G., D. Kolymbas. Constitutive Relations, Some Conclusions from a Workshop, In: Proc. XI ICSMFE, 489-494, San Francisco, Balkema, 1985.

Head, K., 2013. Manual of Soil Laboratory Testing.

Houlsby, G. How the Dilatancy of Soils Affects their Behaviour. In: Proc. 10th ECSMFE, Florence, volume 4, 1189-1202, A. A. Balkema, 1991, Theme lecture.

Jamiolkowski et al. without a losing address. Future trends for penetration testing. Geotechnology Conference - Penetration Testing in the UK, pp. 321-342.

Karstunen, M. Hardening soil model presentation, University of Strathclyde, Glasgow, U.K. 2009

Konrad and Law, 1987b. Undrained shear strength from piezocone tests. Canadian Geotechnical Journal, pp. 392-405.

Kok Sien Ti et al, A review of basic soil constitutive models for geotechnical application, The Electronic Journal of Geotechnical Engineering, University Putra, Malaysia, 2009

Kulhawy and Mayne, 1990. Manual on estimating soil properties for foundation design, Palo Alto, CA: Electric Power Research Institute.

Lacasse, 1986. Dilatometer Tests in Sand.

Lanier, J., C. Di Prisco, R. Nova. Experimental study and theoretical analysis of the induced anisotropy of Hostun sand. Rev. Franc. Geotech, 57 (1991), 59-74, 1991.

Marchetti, Marchetti, S., 1985. On the Field Determination of Ko in Sand. San Francisco, ICSMFE.

Marchetti, S., 2010. Sensitivity of CPT and DMT to stress history and aging in sands for liquefaction assessment, CPT 2010 Int. Symp.

Marchetti, 1980. In situ tests by Flat Dilatometer. Journal of the Geotechnical Engineering Division, 106(GT3), pp. 299-321.

Marcu, A., 1983. Investigation of bedrock and determination of geotechnical design features. Bucharest: Bucharest Institute of Construction.

Oden, J. T., T. Belytschko, I. Babuska, T. Hughes. Research Directions in Computational Mechanics. Computer Methods in Applied Mechanics and Engineering, 192, 913-922, 2003.

Puzrin, A., J. Burland. Non-Linear Model of Small-Strain Behaviour of Soils Geotechnique, 48, No. 2, 217-234, 1998.

Robertson and Campanella, 1983. Interpretation of cone penetration tests. Canadian Geotechnical, J.20(4), pp. 718-745.

Robertson, 2015. Guide to Cone Penetration Testing, 6th Edition, Gregg Drilling & Testing, Inc.

Robertson, 2016. CPT-based Soil Behaviour Type (SBT) Classification System. Canadian Geotechnical Journal.

Robertson, P., 1997. Cone Penetration Test in Geotechnical Practice.

Schanz, T. et al. *The hardening soil model: Formulation and verification*, Conference "Beyond 2000 in Computation Geotechnics", Rotterdam, Nederlands, 1999.

Stallebrass, S., R. Taylor. The Development and Evaluation of a Constitutive Model for the Prediction of Ground Movements in Overconsolidated Clay. Geotechnique, 47, No. 2, 235-253, 1997.

STAS 1913/1-82 Foundation land. Determination of moisture content: ASRO.

STAS 1913/4-86 Foundation land. Determination of plasticity limits. Bucharest: ASRO.

STAS 1913/5-85 Foundation land. Determination of granularity: ASRO.

STAS 8316-77 Founding ground. Fundamental principles of calculation. Bucharest: ASRO.

STAS 8942/1-89 Foundation land. Determination of compressibility of soils by oedometer test. Bucharest: ASRO.

STAS 8942/2-82 Foundation land. Determination of the shear strength of soils by direct shear test. Bucharest: ASRO.

SR EN ISO 22476-3, 2006 Geotechnical investigation and testing - Field testing - Part 1: Electrical cone and piezocone penetration test.



Trofimenkov, 1964. Field Methods for Testing the Structural Properties of Soils. ing Literature Publishing House.

Viggiani, G., J. Atkinson. Interpretation of Bender Element Tests. Geotechnique, 45, No. 1, 149-154, 1995.

Wu, W., E. Bauer. A Simple Hypoplastic Constitutive Model for Sand. International Journal for Numerical and Analytical Methods in Geomechanics, 18, 833-862, 1994.